

Exploration of bifurcation and stability in a class of fractional-order super-double-ring neural network with two shared neurons and multiple delays

Qinrui Dai

School of Mathematics and Statistics, Wuhan University, Wuhan 430072, China



ARTICLE INFO

Keywords:
 Double-ring neural network
 Coates flow graph
 Stability
 Hopf bifurcation

ABSTRACT

Complex multi-ring coupling structures are common in real-world networks. However, the current work is mainly limited to unidirectional multi-ring or those sharing a neuron. This paper is devoted to the stability and Hopf bifurcation of a class of double-ring neural network with two shared neurons and multiple time delays, where n and m neurons are distributed on the double-ring, respectively. First, we obtain the characteristic equation of the network at the trivial equilibrium point by using the Coates flow graph method. Then, based on this, some sufficient conditions for the stability and Hopf bifurcation of the double-ring network under two connection modes are given. Finally, we provide some numerical examples to illustrate the validness of the theoretical results, and the influences of fractional order, network size and the distance between two shared neurons on Hopf bifurcation are also discussed.

1. Introduction

In the past decades, artificial neural networks with excellent signal processing capabilities have been successfully applied to electronic and engineering, including but not limited to computer technology [1,2], artificial intelligence [3,4] and bioengineering [5,6]. The development and practical application of artificial neural networks are inseparable from the dynamics of networks, thus forming the burgeoning interdisciplinary of neurodynamics. For this reason, a large number of recognizable network models are designed to study their nonlinear dynamics, which mainly involve bifurcation, chaos, oscillation, synchronization, etc. For example, Zhang et al. [7] investigated the synchronization and module-phase synchronization phenomenon of a complex-valued neural network by using sliding mode controllers. In [8], a general delayed recurrent neural network is proposed and the local stability and Hopf bifurcation of the network are analyzed. In [9], the chaotic dynamics, such as hyperchaos and transient chaos, in a Hopfield-type neural network with three neurons is studied, and the results of hardware measurement are basically consistent with numerical simulation. It is important to note that the time-lag is usually considered into the modeling of neural networks due to the delay and limited speed of information transmission. Consequently, a great quantity of delayed neural networks more in line with the real-world are established, and the dynamical properties of the network are analyzed with time delay as the key parameter. Meanwhile, since the fractional order is proposed in the 17th century, its mathematical theory has been

gradually improved and widely used in science and engineering. Compared with integer-order dynamical systems, fractional-order systems can more accurately represent phenomena with hereditary and memory characteristics, which makes fractional-order neural networks get great attention in recent years. For instance, α -exponential stability and α -synchronization of a class of fractional-order neural networks are discussed by handling a fractional-order differential inequality in [10]. Xu et al. [11] established a fractional-order neural networks with mixed delays and analyzed the delay-induced periodic oscillation of the network. Huang and Cao [12] investigated a delayed high-order fractional neural networks with multiple neurons for exploring the bifurcation phenomenon induced by the self-feedback delay. In [13], a delayed two-layer coupled fractional-order BAM neural network with $n+2$ neurons is discussed and the existence of Hopf bifurcation for the network is proved.

At present, high-order neural network modeling and ring network architecture innovating have attracted the attention of some scholars. It has been proved that high-dimensional ring structure, especially the multi-ring staggered connection, is widespread in the brain and nervous system [14,15]. Wang et al. [16] discussed a diffusive ring neural network with n neurons and time delay, and then some nontrivial dynamic phenomena, such as synchronized bifurcation, periodic coexistence and bistability, are obtained. In [17], an unidirectional ring neural network with n neurons and distributed delays is established to investigate

E-mail address: daiqinrui@whu.edu.cn.

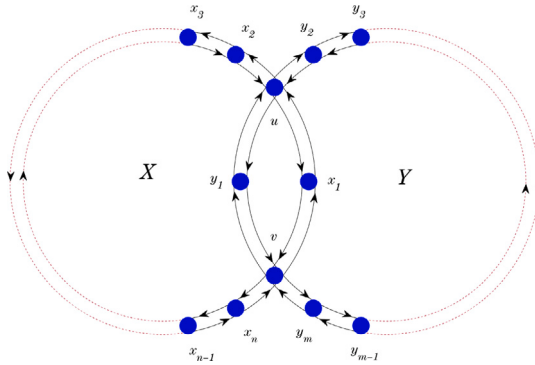


Fig. 1. Schematic diagram of a bidirectional double-ring coupled neural network with two shared neurons.

the stable region and Hopf bifurcation of the network. Notably, Tao et al. [18] studied the stability and bifurcation of a bidirectional ring neural network with multiple delays and n neurons, and first applied Coates flow graph theory to the calculation of characteristic equations of high-dimensional neural networks. Meanwhile, the rise of multi-ring coupled neural networks has brought the ring structure to a new elevation, which is conducive to exploring the complex dynamics of networks. Quintessentially, a unidirectional fractional-order double-ring neural network with multiple delays sharing a neuron is designed to talk over the stability and bifurcation of the network in [19]. Zhang et al. [20] set up an asymmetrical three-ring structured neural network, and the nonlinear oscillations and Hopf Bifurcation of the three-ring network are analyzed, and the influence of neurons and symmetry on the stability of the network is also discussed. Furthermore, based on the study of three-ring, Zhang et al. [21] considered a m -ring coupled fractional-order neural network with a common neuron and multiple delays, and using standard theoretical methods, dynamical bifurcation of the network is investigated.

However, most of the existing multi-ring neural network models are unidirectional information transmission and different rings only share a common neuron node [22–24]. On the one hand, the bidirectional transmission of information is very common in the ecosystem and the real-world [25–27], such as voice calls between people, predator and prey system, servers and clients of the Internet, and nervous system, etc. Therefore, it is natural that a great deal of results have introduced bidirectional interflow into artificial neural network to understand its dynamic mechanism, which requires more complex theoretical calculations in comparison with unidirectional networks. On the other hand, in the process of multi-ring coupling, it is more likely to share two nodes rather than one, that is, the probability of ring intersection is greater than tangent. An obvious example is that the ring-like barbed wire mesh mostly adopts the intersection mode rather than tangent, thus increasing the firmness and stability of the whole network. Accordingly, inspired by the above discussion, we propose a bidirectional double-ring coupled fractional-order neural network with multiple delays, sharing two neuron nodes, as shown in Fig. 1.

The main motivations and contributions of this paper can be summarized as follows:

1. In this paper, a novel double-ring fractional-order neural network with two shared neurons and multiple delays is proposed for the first time.
2. The Coates flow graph method is used to calculate the characteristic equation of the double-ring neural network model, illustrating that this method can be applied to more complex model analysis.
3. We investigate the stability and Hopf bifurcation of bidirectional and unidirectional double-ring networks, and the influence of the fractional order, the number of neurons and the shared positions of the two neurons on the Hopf bifurcation of the network is also discussed.

Compared with the previous results, the theoretical analysis of this paper is more difficult, but we have obtained more abundant theoretical results on the stability of network. In addition, we consider the influence of different factors on the stability of network structure more comprehensively in numerical experiments. Moreover, this kind of double-ring model is more consistent with the real-world ring network interaction and can be extended to more complex network structures, such as multi-ring coupling or even multi-layer-ring network with two shared neurons. The rest of this paper is organized as follows. In Section 2, we give some basic definitions and lemmas for the fractional derivative and calculation of characteristic equation. In Section 3, a novel bidirectional double-ring neural network model with multiple time delays is proposed, and then the stability and Hopf bifurcation of the network are investigated via the characteristic equation induced by the flow graph theory at the trivial equilibrium point. In Section 4, a unidirectional double-ring neural network is considered as a comparative study to analyze its stability and Hopf bifurcation. Section 5 provides some numerical experiments to demonstrate the theoretical results. Finally, a brief conclusions and prospects are addressed in Section 6.

2. Preliminary notes

In this section, some priori knowledge about the fractional differential equations and the Coates flow graph method is given for the convenience of readers.

Define 1 ([28]). *The fractional-order integral of order α for a given function $g(t)$ is defined by*

$${}_t J_t^\alpha g(t) = \frac{1}{\Gamma(\alpha)} \int_{t_0}^t (t-\theta)^{\alpha-1} g(\theta) d\theta, \quad (1)$$

where $\alpha > 0$ and $\Gamma(\cdot)$ is the Gamma function with $\Gamma(s) = \int_0^{+\infty} t^{s-1} e^{-t} dt$.

Define 2 ([28]). *For a given function $g(t) \in C^n [t_0, +\infty)$, the Caputo fractional-order integral of order α is defined as*

$$D^\alpha g(t) = \frac{1}{\Gamma(n-\alpha)} \int_{t_0}^t (t-\theta)^{n-\alpha-1} g^{(n)}(\theta) d\theta, \quad (2)$$

where $n-1 < \alpha < n$ ($n \in \mathbb{Z}^+$).

Consider the following m -dimensional linear fractional differential system with multiple time delays:

$$\begin{cases} D^{\alpha_1} x_1(t) = a_{11}x_1(t - \sigma_{11}) + \dots + a_{1m}x_m(t - \sigma_{1m}), \\ D^{\alpha_2} x_2(t) = a_{21}x_1(t - \sigma_{21}) + \dots + a_{2m}x_m(t - \sigma_{2m}), \\ \vdots \\ D^{\alpha_m} x_m(t) = a_{m1}x_1(t - \sigma_{m1}) + \dots + a_{mm}x_m(t - \sigma_{mm}), \end{cases} \quad (3)$$

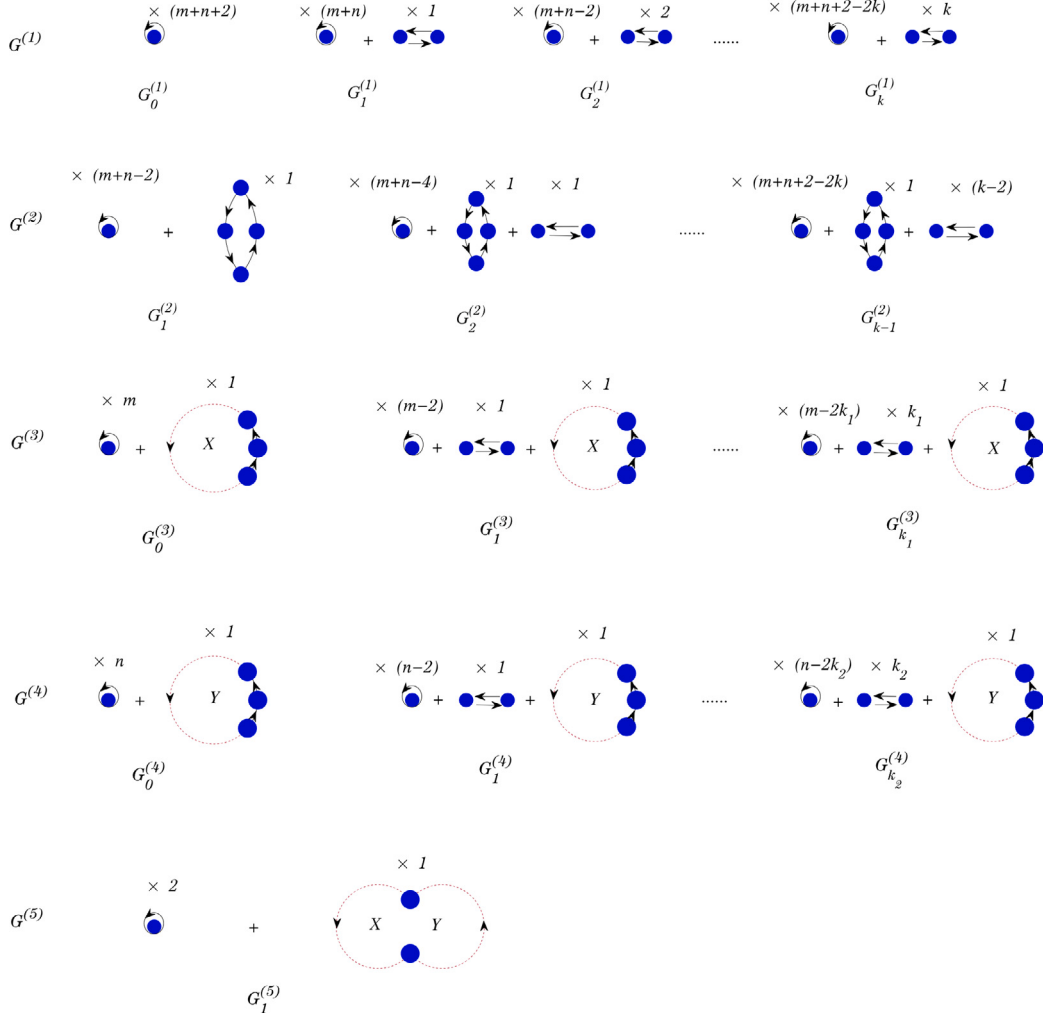


Fig. 2. The $2k + k_1 + k_2 + 3$ classifications of flow graph G associated with the matrix $\Delta(\lambda)$.

where $0 < \alpha_i \leq 1$ and $\sigma_{ij} > 0$ for $i, j = 1, 2, \dots, m$. The characteristic equation of (3) is given by

$$\Delta(\lambda, \sigma) = \begin{vmatrix} \lambda^{\alpha_1} - a_{11}e^{-\lambda\sigma_{11}} & \cdots & -a_{1m}e^{-\lambda\sigma_{1m}} \\ \vdots & \ddots & \vdots \\ -a_{m1}e^{-\lambda\sigma_{m1}} & \cdots & \lambda^{\alpha_m} - a_{mm}e^{-\lambda\sigma_{mm}} \end{vmatrix}_{m \times m} = 0. \quad (4)$$

Lemma 1 ([29]). For linear system (3), the following two statements are true

1. If system (3) has a unique zero solution, then the zero solution of (3) is Lyapunov globally asymptotically stable when all the roots of the characteristic equation (4) have negative real parts.
2. In particular, for all $\alpha_i = \alpha$ and $\sigma_{ij} = 0$ ($i, j = 1, 2, \dots, m$), the zero solution of (3) is Lyapunov globally asymptotically stable if and only if the arguments of all the roots λ of Eq. (5) satisfy $|\arg(\lambda)| > \frac{\alpha\pi}{2}$, in which

$$\Delta'(\lambda) = \begin{vmatrix} \lambda^\alpha - a_{11} & \cdots & -a_{1m} \\ \vdots & \ddots & \vdots \\ -a_{m1} & \cdots & \lambda^\alpha - a_{mm} \end{vmatrix}_{m \times m} = 0. \quad (5)$$

Lemma 2 ([30]). For a n -order square matrix Q corresponding to a flow graph G , the determinant of G is determined by

$$\det Q = \sum_{i=1}^p (-1)^{n+n_i} G_i,$$

where p represents the types of non-contact loop. n_i and G_i are the number of directed loops and the connection gain in the i th type of non-contact loop ($i = 1, \dots, p$).

Remark 1. The traditional matrix operator is no longer applicable to the calculation of characteristic equations of high-dimensional systems with complex parameters. The authors in [30] proposed a novel Coates flow graph method to calculate the determinant of matrix. Subsequently, Tao et al. [18] applied this method to calculate the characteristic equation of high-dimensional ring network for the first time and achieved great success.

3. Local stability and Hopf bifurcation

In this section, a general bidirectional double-ring neural network model is established, and its characteristic equation is obtained by means of Coates flow graph method. Then the stability and Hopf bifurcation of the network with and without time delay are investigated based on the characteristic equation.

The mathematical expression of asymmetric bidirectional double-ring coupled fractional-order neural network is as follows:

$$\begin{aligned}
D^\alpha u(t) &= -a_u u(t) + b_{1u}^1 f_{1u}^1(x_1(t - \tau_{1u}^1)) + b_{2u}^1 f_{2u}^1(x_2(t - \tau_{2u}^1)) \\
&\quad + b_{1u}^2 f_{1u}^2(y_1(t - \tau_{1u}^2)) + b_{2u}^2 f_{2u}^2(y_2(t - \tau_{2u}^2)), \\
D^\alpha v(t) &= -a_v v(t) + b_{1v}^1 f_{1v}^1(x_1(t - \tau_{1v}^1)) + b_{nv}^1 f_{nv}^1(x_n(t - \tau_{nv}^1)) \\
&\quad + b_{1v}^2 f_{1v}^2(y_1(t - \tau_{1v}^2)) + b_{mv}^2 f_{mv}^2(y_m(t - \tau_{mv}^2)), \\
D^\alpha x_1(t) &= -a_1^1 x_1(t) + b_{u1}^1 f_{u1}^1(u(t - \tau_{u1}^1)) + b_{v1}^1 f_{v1}^1(v(t - \tau_{v1}^1)), \\
D^\alpha y_1(t) &= -a_1^2 y_1(t) + b_{u1}^2 f_{u1}^2(u(t - \tau_{u1}^2)) + b_{v1}^2 f_{v1}^2(v(t - \tau_{v1}^2)), \\
D^\alpha x_2(t) &= -a_2^1 x_2(t) + b_{32}^1 f_{32}^1(x_3(t - \tau_{32}^1)) + b_{u2}^1 f_{u2}^1(u(t - \tau_{u2}^1)), \\
D^\alpha y_2(t) &= -a_2^2 y_2(t) + b_{32}^2 f_{32}^2(y_3(t - \tau_{32}^2)) + b_{u2}^2 f_{u2}^2(u(t - \tau_{u2}^2)), \\
D^\alpha x_i(t) &= -a_i^1 x_i(t) + b_{(i-1)i}^1 f_{(i-1)i}^1(x_{i-1}(t - \tau_{(i-1)i}^1)) \\
&\quad + b_{(i+1)i}^1 f_{(i+1)i}^1(x_{i+1}(t - \tau_{(i+1)i}^1)), \\
D^\alpha y_j(t) &= -a_j^2 y_j(t) + b_{(j-1)j}^2 f_{(j-1)j}^2(y_{j-1}(t - \tau_{(j-1)j}^2)) \\
&\quad + b_{(j+1)j}^2 f_{(j+1)j}^2(y_{j+1}(t - \tau_{(j+1)j}^2)), \\
D^\alpha x_n(t) &= -a_n^1 x_n(t) + b_{vn}^1 f_{vn}^1(v(t - \tau_{vn}^1)) + b_{(n-1)n}^1 f_{(n-1)n}^1 \\
&\quad \times (x_{n-1}(t - \tau_{(n-1)n}^1)), \\
D^\alpha y_m(t) &= -a_m^2 y_m(t) + b_{vm}^2 f_{vm}^2(v(t - \tau_{vm}^2)) + b_{(m-1)m}^2 f_{(m-1)m}^2 \\
&\quad \times (y_{m-1}(t - \tau_{(m-1)m}^2)),
\end{aligned} \tag{6}$$

where $i = 3, 4, \dots, n-1$, $j = 3, 4, \dots, m-1$. n and m represent the number of neurons on X -ring and Y -ring except for two shared neurons, respectively; $a_u, a_v, a_i^1, a_i^2, a_n^1, a_n^2$ are the self-feedback coefficient of neurons u, v, x_i, y_j, x_n, y_m ; $b_{(i-1)i}^1$ (or $b_{(j-1)j}^2$) stands for the connection weight between neuron x_{i-1} (or y_{j-1}) and x_i (or y_j), accompanied by the activation function $f_{(i-1)i}^1$ (or $f_{(j-1)j}^2$) of x_{i-1} (or y_{j-1}). Similarly, other weight parameters and activation functions have the same meaning as $b_{(i-1)i}^1$ and $f_{(i-1)i}^1$, for example, b_{1u}^1 (or b_{vn}^2) denotes the connection weight between x_1 (or v) and u (or y_n), accompanied by the activation function f_{1u}^1 (or f_{vn}^1) of x_1 (or v); $\tau_{(i-1)i}^1$ (or $\tau_{(j-1)j}^2$) represents the time delay of information transmission between x_{i-1} (or y_{j-1}) and x_i (or y_j), similar to other delays.

Remark 2. The node dynamics, such as the shared node u , there are four neurons (x_1, y_1, x_2, y_2) transmitting information to it, so the change of the state of neuron u is affected by x_1, y_1, x_2 and y_2 . The purpose of activation function is to add some nonlinear factors to the neural network, so that the neural network can better solve more complex problems. Therefore, nonlinear function $f(x) = \tanh(x)$ is generally selected as the activation function.

Remark 3. According to the distance (that is, the number of neurons) between two shared neurons on different ring, there are $\lfloor \frac{n}{2} \rfloor \times \lfloor \frac{m}{2} \rfloor$ different topological patterns in the double-ring neural network. It is worth mentioning that there are two distances between two neurons on a ring, only the smaller one needs to be considered. Nevertheless, network (6) is a relatively simple one, that is, only one neuron is separated between two shared neurons on the X -ring and the Y -ring. (Eq. (7) is given in Box I, where the coefficients are actually redefined. For example, $b_{ij} f_{ij}'(0)$ is rewritten as b_{ij})

As a matter of convenience, some necessary hypotheses need to be listed below,

(H1) :

$$f_{1u}^1, f_{1v}^1, \dots, f_{vn}^1, f_{nv}^1 \in C(R, R), f_{1u}^2, f_{1v}^2, \dots, f_{vm}^2, f_{mv}^2 \in C(R, R),$$

$$f_{1u}^1(0) = f_{u1}^1(0) = \dots = f_{nv}^1(0) = f_{vn}^1(0) = 0,$$

$$f_{1u}^2(0) = f_{u1}^2(0) = \dots = f_{mv}^2(0) = f_{vm}^2(0) = 0,$$

$$(f_{1u}^1)'(0), (f_{u1}^1)'(0), \dots, (f_{nv}^1)'(0), (f_{vn}^1)'(0) \neq 0,$$

$$(f_{1u}^2)'(0), (f_{u1}^2)'(0), \dots, (f_{mv}^2)'(0), (f_{vm}^2)'(0) \neq 0,$$

$$a_u = a_v = \dots = a_n^1 = a_m^2 = a.$$

(H2) :

$$\tau_{1u}^1 + \tau_{u1}^1 = \tau_{2u}^1 + \tau_{u2}^1 = \tau_{1v}^1 + \tau_{v1}^1 = \tau_{nv}^1 + \tau_{vn}^1 = \tau_{i(i+1)}^1 + \tau_{i(i+1)}^1 = 2\tau,$$

$$\tau_{1u}^2 + \tau_{u1}^2 = \tau_{2u}^2 + \tau_{u2}^2 = \tau_{1v}^2 + \tau_{v1}^2 = \tau_{mv}^2 + \tau_{vm}^2 = \tau_{j(j+1)}^2 + \tau_{j(j+1)}^2 = 2\tau.$$

(H3) :

$$\tau_{nv}^1 + \tau_{v1}^1 + \tau_{1u}^1 + \tau_{u2}^1 + \sum_{i=2}^{n-1} \tau_{i(i+1)}^1 = (n+2)\tau,$$

$$\tau_{mv}^2 + \tau_{v1}^2 + \tau_{1u}^2 + \tau_{u2}^2 + \sum_{j=2}^{m-1} \tau_{j(j+1)}^2 = (m+2)\tau,$$

$$\tau_{nv}^1 + \tau_{u2}^1 + \tau_{mv}^2 + \tau_{u2}^2 + \sum_{i=2}^{n-1} \tau_{i(i+1)}^1 + \sum_{j=2}^{m-1} \tau_{j(j+1)}^2 = (n+m)\tau,$$

$$\tau_{1u}^1 + \tau_{u1}^2 + \tau_{1v}^2 + \tau_{v1}^1 = 4\tau.$$

Remark 4. Since the high-dimensional network system contains a large number of parameters, usually some restrictive assumptions need to be given to simplify the calculation. More specifically, (H1) is a hypothesis for the activation functions and self-feedback coefficients, which guarantees the regularity of the linearization system of the network. (H2) and (H3) are the constraints on the network delays, which means that the sum of the delays of any two neurons with bidirectional connection is 2τ , and the sum of the delays on any unidirectional ring is the number of its neurons multiplied by τ .

Now, we try to calculate the characteristic equation of network (6) based on Lemma 2. To this end, let $\Delta(\lambda)$ shown in Eq. (7) be the matrix corresponding to Coates flow graph G . It is easy to check from Fig. 2 that all subgraphs of G are divided into $2k + k_1 + k_2 + 3$ types of non-contact ring, where $k = \lfloor \frac{n+m+2}{2} \rfloor$, $k_1 = \lfloor \frac{n-1}{2} \rfloor$ and $k_2 = \lfloor \frac{m-1}{2} \rfloor$. Consequently, all subgraphs of G can be regarded as a set defined by $E = \{G_0^{(1)}, G_1^{(1)}, G_2^{(1)}, \dots, G_k^{(1)}, G_1^{(2)}, G_2^{(2)}, \dots, G_{k-1}^{(2)}, G_0^{(3)}, G_1^{(3)}, \dots, G_{k_1}^{(3)}, G_0^{(4)}, G_1^{(4)}, \dots, G_{k_2}^{(4)}, G_1^{(5)}\}$, each element of which also contains those similar subgraphs. To be more specific, all elements of E can be summarized as follows:

1. $G^{(1)} = \{G_0^{(1)}, G_1^{(1)}, \dots, G_k^{(1)}\}$, where $G_i^{(1)}$ ($i = 0, 1, \dots, k$) represents the set of all subgraphs with $n+m+2-i$ loops, including $n+m+2-2i$ self-loops and i double-neuron-loops.
2. $G^{(2)} = \{G_1^{(2)}, G_2^{(2)}, \dots, G_{k-1}^{(2)}\}$, where $G_i^{(2)}$ ($i = 1, \dots, k-1$) denotes the set of all subgraphs with $n+m-j$ loops, involving $n+m-2i$ self-loops, $i-1$ double-neuron-loops and 1 four-neuron-loop.
3. $G^{(3)} = \{G_0^{(3)}, G_1^{(3)}, \dots, G_{k_1}^{(3)}\}$, where $G_i^{(3)}$ ($i = 0, \dots, k_1$) is the set of all subgraphs with $m+1-i$ loops, containing $m-2i$ self-loops, i double-neuron-loops and 1 $(n+2)$ -neuron-loop.
4. $G^{(4)} = \{G_0^{(4)}, G_1^{(4)}, \dots, G_{k_2}^{(4)}\}$, where $G_i^{(4)}$ ($i = 0, \dots, k_2$) is the set of all subgraphs with $n+1-i$ loops, involving $n-2i$ self-loops, i double-neuron-loops and 1 $(m+2)$ -neuron-loop.
5. $G^{(5)} = \{G_1^{(5)}\}$, where $G_1^{(5)}$ stands for the set of all subgraphs with 3 loops, this is, 2 self-loops and 1 $(n+m)$ -neuron-loop.

For convenience of description, define $c_1 = b_{1u}^1 b_{u1}^1$, $c_2 = b_{u2}^1 b_{2u}^1$, $c_i = b_{(i-1)i}^1 b_{i(i-1)}^1$, $c_{n+1} = b_{nv}^1 b_{vn}^1$, $c_{n+2} = b_{1v}^1 b_{v1}^1$, $d_1 = b_{1u}^2 b_{u1}^2$, $d_2 = b_{u2}^2 b_{2u}^2$,

$$\Delta(\lambda) =$$

$$\left(\begin{array}{ccccccccc} \lambda^\alpha + a_u & 0 & -b_{1u}^1 e^{-\lambda \tau_{1u}} & \dots & 0 & -b_{1u}^2 e^{-\lambda \tau_{1u}^2} & -b_{2v}^2 e^{-\lambda \tau_{2v}^2} & \dots & 0 \\ 0 & \lambda^\alpha + a_v & -b_{1v}^1 e^{-\lambda \tau_{1v}} & \dots & -b_{nv}^1 e^{-\lambda \tau_{nv}} & -b_{1v}^2 e^{-\lambda \tau_{1v}^2} & 0 & \dots & -b_{mv}^2 e^{-\lambda \tau_{mv}^2} \\ -b_{u1}^1 e^{-\lambda \tau_{u1}^1} & -b_{v1}^1 e^{-\lambda \tau_{v1}^1} & \lambda^\alpha + a_1^1 & \dots & 0 & 0 & 0 & \dots & 0 \\ \vdots & \vdots & \vdots & \ddots & \vdots & \vdots & \vdots & \dots & \vdots \\ 0 & -b_{vn}^1 e^{-\lambda \tau_{vn}^1} & 0 & \dots & \lambda^\alpha + a_n^1 & 0 & 0 & \dots & 0 \\ -b_{u1}^2 e^{-\lambda \tau_{u1}^2} & -b_{v1}^2 e^{-\lambda \tau_{v1}^2} & 0 & \dots & 0 & \lambda^\alpha + a_1^2 & 0 & \dots & 0 \\ -b_{u2}^2 e^{-\lambda \tau_{u2}^2} & 0 & 0 & \dots & 0 & 0 & \lambda^\alpha + a_2^2 & \dots & 0 \\ \vdots & \vdots & \vdots & \ddots & \vdots & \vdots & \vdots & \ddots & \vdots \\ 0 & 0 & 0 & \dots & 0 & 0 & 0 & \dots & \lambda^\alpha + a_{m-1}^2 \\ 0 & -b_{vm}^2 e^{-\lambda \tau_{vm}^2} & 0 & \dots & 0 & 0 & 0 & \dots & -b_{(m-1)m}^2 e^{-\lambda \tau_{(m-1)m}^2} \\ \end{array} \right) \quad (7)$$

Box I.

$d_j = b_{(j-1)j}^2 b_{j(j-1)}^2$, $d_{m+1} = b_{mv}^2 b_{vm}^2$, $d_{m+2} = b_{1v}^2 b_{v1}^2$ with $i = 3, 4, \dots, n, j = 3, 4, \dots, m$. Hence, for each element of E , we have the following product of the each side for the subgraphs in view of Lemma 2 and hypotheses (H2) – (H3),

$$\begin{aligned} Q_0^{(1)} &= (-1)^{n+m+2} (\lambda^\alpha + a)^{n+m+2}, \\ Q_1^{(1)} &= (-1)^{n+m+1} (\lambda^\alpha + a)^{n+m} \varphi_1^{(1)} e^{-2\lambda\tau}, \\ Q_2^{(1)} &= (-1)^{n+m} (\lambda^\alpha + a)^{n+m-2} \varphi_2^{(1)} e^{-4\lambda\tau}, \\ &\vdots \\ Q_k^{(1)} &= (-1)^{n+m+2-k} (\lambda^\alpha + a)^{n+m+2-2k} \varphi_k^{(1)} e^{-2k\lambda\tau}, \\ Q_0^{(2)} &= (-1)^{n+m-1} (\lambda^\alpha + a)^{n+m-2} \varphi_1^{(2)} e^{-4\lambda\tau}, \\ Q_2^{(2)} &= (-1)^{n+m-2} (\lambda^\alpha + a)^{n+m-4} \varphi_2^{(2)} e^{-6\lambda\tau}, \\ &\vdots \\ Q_{k-1}^{(2)} &= (-1)^{n+m+1-k} (\lambda^\alpha + a)^{n+m+2-2k} \varphi_k^{(2)} e^{-2k\lambda\tau}, \\ Q_0^{(3)} &= (-1)^{m+1} (\lambda^\alpha + a)^m \varphi_0^{(3)} e^{-(n+2)\lambda\tau}, \\ Q_1^{(3)} &= (-1)^m (\lambda^\alpha + a)^{m-2} \varphi_1^{(3)} e^{-(n+4)\lambda\tau}, \\ &\vdots \\ Q_{k_1}^{(3)} &= (-1)^{m+1-k_1} (\lambda^\alpha + a)^{m-2k_1} \varphi_{k_1}^{(3)} e^{-(n+2k_1+2)\lambda\tau}, \\ Q_0^{(4)} &= (-1)^{n+1} (\lambda^\alpha + a)^n \varphi_0^{(4)} e^{-(m+2)\lambda\tau}, \\ Q_1^{(4)} &= (-1)^n (\lambda^\alpha + a)^{n-2} \varphi_1^{(4)} e^{-(m+4)\lambda\tau}, \\ &\vdots \\ Q_{k_2}^{(4)} &= (-1)^{n+1-k_2} (\lambda^\alpha + a)^{n-2k_2} \varphi_{k_2}^{(4)} e^{-(m+2k_2+2)\lambda\tau}, \\ Q_1^{(5)} &= (-1)^3 (\lambda^\alpha + a)^2 \varphi_1^{(5)} e^{-(n+m)\lambda\tau}, \end{aligned}$$

where $Q_j^{(j)}$ represents the connection gain in the j th type of non-contact loop $G^{(j)}$ with $j = 1, 2, 3, 4, 5$; The parameters $\varphi_1^{(1)}, \varphi_2^{(1)}, \dots, \varphi_k^{(1)}, \varphi_1^{(2)}, \dots, \varphi_{k-1}^{(2)}, \varphi_0^{(3)}, \varphi_1^{(3)}, \dots, \varphi_{k_1}^{(3)}, \varphi_0^{(4)}, \varphi_1^{(4)}, \dots, \varphi_{k_2}^{(4)}, \varphi_1^{(5)}$ are located in the Appendix at the end of the paper.

Finally, we can obtain the characteristic equation of network (6) at the trivial equilibrium point

$$\det \Delta(\lambda) = (-1)^{n+m+2} \left(\sum_{j=0}^k Q_j^{(1)} + \sum_{j=1}^{k-1} Q_j^{(2)} + \sum_{j=0}^{k_1} Q_j^{(3)} + \sum_{j=0}^{k_2} Q_j^{(4)} + Q_1^{(5)} \right) = 0.$$

Further substituting the corresponding target into the above formula, the following specific form can be obtained

$$\begin{aligned} &(\lambda^\alpha + a)^{n+m+2} + \sum_{j=1}^k (-1)^j \varphi_j^{(1)} (\lambda^\alpha + a)^{n+m+2-2j} e^{-2j\lambda\tau} \\ &+ \sum_{j=1}^{k-1} (-1)^j \varphi_j^{(2)} (\lambda^\alpha + a)^{n+m+2-2(j+1)} e^{-2(j+1)\lambda\tau} \\ &+ \sum_{j=0}^{k_1} (-1)^{n+j} \varphi_j^{(3)} (\lambda^\alpha + a)^{m-2(j+1)} e^{-(n+2+2(j-1))\lambda\tau} \\ &+ \sum_{j=0}^{k_2} (-1)^{m+j} \varphi_j^{(4)} (\lambda^\alpha + a)^{n-2(j+1)} e^{-(m+2+2(j-1))\lambda\tau} \\ &+ (-1)^{n+m+1} \varphi_1^{(5)} (\lambda^\alpha + a)^2 e^{-(n+m)\lambda\tau} = 0. \end{aligned} \quad (8)$$

Remark 5. In fact, compared with the previous ring neural network model, the characteristic equation (8) is a more complex transcendental equation with multiple exponential terms. For example, in the bidirectional single-ring model [18] and the single-ring model with ring-hub structure [31], their characteristic equations have only two kinds of exponential terms, while Eq. (8) has five kinds of exponential terms. Therefore, it is more difficult to study the root distribution of Eq. (8) using the standard theory.

Remark 6. Due to the increase of the exponential term, the numerical solution of the characteristic equation root of our network is more difficult to calculate, but in fact, our network has more abundant dynamic phenomena, such as alternating stable intervals, more Hopf bifurcations, and more likely Hopf-Hopf bifurcations. Moreover, the network model in [31] does not study the way of information transmission, which is also very important for exploring network dynamics.

Next, based on the distribution of the roots of the characteristic equation (8), we investigate the local stability and Hopf bifurcation of the asymmetric bidirectional double-ring neural network model (6) at the trivial equilibrium point.

3.1. Case without time delay ($\tau = 0$)

In this case, the characteristic equation (8) is equivalent to

$$s^{n+m+2} + \sum_{i=1}^{n+m+2} A_i s^{n+m+2-i} = 0, \quad (9)$$

where $s = \lambda^\alpha$ and

$$A_i = \begin{cases} B_i + F_i, & n+m+2 \geq i > n, m. \quad \text{or} \quad n+m+2 \geq i \geq n+m \\ B_i + D_i, & m \geq i > n \\ B_i + E_i, & n \geq i > m \\ B_i + E_i + D_i, & i \leq n, m \end{cases}$$

in which

$$F_i = (-1)^{n+m+1} C_2^{n+m+2-k} a^{n+m+2-k},$$

$$B_i = \left\{ C_{n+m+2}^i a^i + \sum_{j=1}^k \left[h(i-2j)(-1)^j \varphi_j^{(1)} C_{n+m+2-j}^{i-2j} a^{i-2j} \right] \right. \\ \left. + \sum_{j=1}^{k-1} \left[h(i-2(j+1))(-1)^j \varphi_j^{(2)} C_{n+m+2-2(j+1)}^{i-2(j+1)} a^{i-2(j+1)} \right] \right\},$$

$$D_i = \sum_{j=0}^{k_1} \left[h(i-2(j+1))(-1)^{n+j} \varphi_j^{(3)} C_{m-2(j+1)}^{i-2(j+1)} a^{i-2(j+1)} \right],$$

$$E_i = \sum_{j=0}^{k_2} \left[h(i-2(j+1))(-1)^{m+j} \varphi_j^{(4)} C_{n-2(j+1)}^{i-2(j+1)} a^{i-2(j+1)} \right],$$

with

$$h(t) = \begin{cases} 1, & t \geq 0 \\ 0, & t < 0. \end{cases}$$

Defining

$$H_i = \begin{vmatrix} A_1 & A_3 & A_5 & \cdots & A_{2i-1} \\ 1 & A_2 & A_4 & \cdots & A_{2i-2} \\ 0 & A_1 & A_3 & \cdots & A_{2i-3} \\ \vdots & \vdots & \vdots & \ddots & \vdots \\ 0 & 0 & 0 & \cdots & A_i \end{vmatrix} \quad i = 1, 2, \dots, n+m+2,$$

one obtains

Lemma 3. For $\tau = 0$, the trivial equilibrium point of network (6) is locally asymptotically stable when all $H_i > 0$, $i = 1, 2, \dots, n+m+2$.

Proof. According to the Routh–Hurwitz criterion, it is obvious that if all $H_i > 0$, $i = 1, 2, \dots, n+m+2$, then all roots of Eq. (9) have negative real parts, that is, the arguments of the root s satisfies $|\arg(s)| > \frac{\alpha\pi}{2}$. Consequently, on account of Lemma 1, the trivial equilibrium point of network (6) is locally asymptotically stable.

3.2. Case with time delay ($\tau > 0$)

In this case, to simplify the analysis, multiplying both sides of Eq. (8) by $e^{(n+m+2)\lambda\tau}$ leads to

$$s^{n+m+2} + \sum_{j=1}^k (-1)^j \varphi_j^{(1)} s^{n+m+2-2j} + \sum_{j=0}^{k-1} (-1)^j \varphi_j^{(2)} s^{n+m+2-2(j+1)} \\ + \sum_{j=0}^{k_1} (-1)^{n+j} \varphi_j^{(3)} s^{m-2(j+1)} \\ + \sum_{j=0}^{k_2} (-1)^{m+j} \varphi_j^{(4)} s^{n-2(j+1)} + (-1)^{n+m+1} \varphi_1^{(5)} s^2 = 0, \quad (10)$$

where $s = (\lambda^\alpha + a) e^{\lambda\tau}$. We know that the form of Eq. (10) is a $(n+m+2)$ -order equation with constant coefficients of all orders. Hence, there are $n+m+2$ roots in Eq. (10) defined as $S_r = \xi_r + i\gamma_r$, $r = 1, 2, \dots, n+m+2$, which shows

$$(\lambda^\alpha + a) e^{\lambda\tau} = \xi_r + i\gamma_r. \quad (11)$$

Suppose that $\lambda = \pm i\omega(\omega > 0)$ is a pair of pure imaginary roots of Eq. (10). Then, $\lambda = i\omega(\omega > 0)$ is also a root of Eq. (11) if and only if

$$\left[\omega^\alpha \left(\cos \frac{\alpha\pi}{2} + i \sin \frac{\alpha\pi}{2} \right) + a \right] (\cos \omega\tau + i \sin \omega\tau) = \xi_r + i\gamma_r.$$

Separating the real part and imaginary part of the upper equation, we have

$$\left\{ \begin{array}{l} \cos \omega\tau = \frac{\xi_r \left(\omega^\alpha \cos \frac{\alpha\pi}{2} + a \right) + \gamma_r \omega^\alpha \sin \frac{\alpha\pi}{2}}{\left(\omega^\alpha \cos \frac{\alpha\pi}{2} + a \right)^2 + \left(\omega^\alpha \sin \frac{\alpha\pi}{2} \right)^2} \triangleq p(\omega) \\ \sin \omega\tau = \frac{\gamma_r \left(\omega^\alpha \cos \frac{\alpha\pi}{2} + a \right) - \xi_r \omega^\alpha \sin \frac{\alpha\pi}{2}}{\left(\omega^\alpha \cos \frac{\alpha\pi}{2} + a \right)^2 + \left(\omega^\alpha \sin \frac{\alpha\pi}{2} \right)^2} \triangleq q(\omega). \end{array} \right.$$

Following the fact $\sin^2 \omega\tau + \cos^2 \omega\tau = 1$ receives

$$\psi(\omega) \triangleq \omega^{2\alpha} + 2a\omega^\alpha \cos \frac{\alpha\pi}{2} + a^2 - \xi_r^2 - \gamma_r^2 = 0. \quad (12)$$

For Eq. (12), we have the following result.

Lemma 4. If $a < |S_{r_0}|$ holds for existing $r_0 \in \{1, 2, \dots, n+m+2\}$, then Eq. (12) has at least one positive root, that is, Eq. (10) has at least one pair of purely imaginary roots.

Proof. It is clear that the function $\psi(\omega)$ is a continuous function with respect to ω on $[0, +\infty)$ and $\lim_{\omega \rightarrow +\infty} \psi(\omega) = +\infty$. Thus, if there is a $r_0 \in \{1, 2, \dots, n+m+2\}$ such that $a < |S_{r_0}|$ holds, then $\psi(0) = a^2 - \xi_{r_0}^2 - \gamma_{r_0}^2 = a^2 - S_{r_0}^2 < 0$. According to the zero point theorem, we can know that there must be a positive number ω , which satisfies $\psi(\omega) = 0$, that is, ω is a root of Eq. (12).

Without lose of generality, it is assumed that there are $n+m+2$ roots in Eq. (12) denoted as ω_r ($r = 1, 2, \dots, n+m+2$). Hence, the critical value τ of Hopf bifurcation is given by

$$\tau_r^{(j)} = \frac{1}{\omega_r} \{ \arccos p(\omega_r) + 2j\pi \}, j = 0, 1, 2, \dots$$

Let $\tau_0 = \tau_{r_0}^{(0)} = \min_{r=1, \dots, n+m+2} \{ \tau_r^{(0)} \}$ with the critical frequency $\omega_0 = \omega_{r_0}$. Up to now, in order to ensure that network (6) undergoes a Hopf bifurcation, the transversality condition is further investigated in accordance with the following steps. Differentiating both sides of Eq. (10) with respect to τ yields

$$\alpha \lambda^{\alpha-1} \frac{d\lambda}{d\tau} + (\lambda^\alpha + a) \left(\frac{d\lambda}{d\tau} \tau + \lambda \right) = 0,$$

clearly,

$$\left(\frac{d\lambda}{d\tau} \right)^{-1} = -\frac{\alpha \lambda^{\alpha-2}}{\lambda^\alpha + a} - \frac{\tau}{\lambda}.$$

Then,

$$\operatorname{sign} \left(\frac{d\lambda}{d\tau} \right)_{\lambda=i\omega_0, \tau=\tau_0}^{-1} = \operatorname{sign} \left(\frac{M_1 N_1 + M_2 N_2}{M_1^2 + M_2^2} \right),$$

where

$$M_1 = \omega_0^\alpha \cos \frac{\alpha\pi}{2} + a, M_2 = \omega_0^\alpha \sin \frac{\alpha\pi}{2},$$

$$N_1 = -\alpha \omega_0^{\alpha-2} \cos \frac{(\alpha-2)\pi}{2},$$

$$N_2 = -\alpha \omega_0^{\alpha-2} \sin \frac{(\alpha-2)\pi}{2}.$$

Making the hypothesis

$$(H4) : M_1 N_1 + M_2 N_2 > 0,$$

we have the following theorem.

Theorem 1. If hypothesis (H4) and the condition of Lemma 4 are true, then the trivial equilibrium of network (6) is locally asymptotically stable when $\tau \in [0, \tau_0]$, and unstable when $\tau > \tau_0$. In particular, network (6) undergoes a Hopf bifurcation at the trivial equilibrium when $\tau = \tau_r^{(j)}$ for $r = 1, 2, \dots, n+m+2$, $j = 0, 1, 2, \dots$

4. Unidirectional double-ring model

In this section, we consider a unidirectional double-ring neural network model with multiple delays, that is, compared with network (6), the information transmission of the network on each ring is unidirectional, corresponding to the following mathematical expression

$$\begin{aligned} D^\alpha u(t) &= -a_u u(t) + b_{1u}^1 f_{1u}^1(x_1(t - \tau_{1u}^1)) + b_{1u}^2 f_{1u}^2(y_1(t - \tau_{1u}^2)), \\ D^\alpha v(t) &= -a_v v(t) + b_{nv}^1 f_{nv}^1(x_n(t - \tau_{nv}^1)) + b_{nv}^2 f_{nv}^2(y_m(t - \tau_{nv}^2)), \\ D^\alpha x_1(t) &= -a_1^1 x_1(t) + b_{v1}^1 f_{v1}^1(v(t - \tau_{v1}^1)), \\ D^\alpha y_1(t) &= -a_1^2 y_1(t) + b_{v1}^2 f_{v1}^2(v(t - \tau_{v1}^2)), \\ D^\alpha x_2(t) &= -a_2^1 x_2(t) + b_{u2}^1 f_{u2}^1(u(t - \tau_{u2}^1)), \\ D^\alpha y_2(t) &= -a_2^2 y_2(t) + b_{u2}^2 f_{u2}^2(u(t - \tau_{u2}^2)), \\ D^\alpha x_i(t) &= -a_{i-1}^1 x_i(t) + b_{(i-1)i}^1 f_{(i-1)i}^1(x_{i-1}(t - \tau_{(i-1)i}^1)), \\ D^\alpha y_j(t) &= -a_{j-1}^2 y_j(t) + b_{(j-1)j}^2 f_{(j-1)j}^2(y_{j-1}(t - \tau_{(j-1)j}^2)), \\ D^\alpha x_n(t) &= -a_{n-1}^1 x_n(t) + b_{(n-1)n}^1 f_{(n-1)n}^1(x_{n-1}(t - \tau_{(n-1)n}^1)), \\ D^\alpha y_m(t) &= -a_{m-1}^2 y_m(t) + b_{(m-1)m}^2 f_{(m-1)m}^2(y_{m-1}(t - \tau_{(m-1)m}^2)), \end{aligned} \quad (13)$$

where the meanings of variables and parameters are the same as those in network (6). Compared with network (6), the information received by each neuron of network (13) is reduced by half, and its dynamics is more concise. Clearly, network (13) has a trivial equilibrium point and based on hypothesis (H1)–(H3) and the aid of the flow graph method, the characteristic equation of the network at this equilibrium point is as follows

$$\begin{aligned} (\lambda^\alpha + a)^{n+m+2} - (\phi_1 + \phi_2)(\lambda^\alpha + a)^n e^{-\lambda(m+2)\tau} \\ - (\phi_3 + \phi_4)(\lambda^\alpha + a)^m e^{-\lambda(n+2)\tau} = 0, \end{aligned} \quad (14)$$

in which

$$\begin{aligned} \phi_1 &= b_{nv}^1 b_{v1}^1 b_{1u}^1 b_{u2}^1 \prod_{i=2}^{n-1} b_{i(i+1)}^1, \quad \phi_2 = b_{nv}^1 b_{v1}^2 b_{1u}^2 b_{u2}^1 \prod_{i=2}^{n-1} b_{i(i+1)}^1, \\ \phi_3 &= b_{nv}^2 b_{v1}^2 b_{1u}^2 b_{u2}^2 \prod_{j=2}^{m-1} b_{j(j+1)}^2, \quad \phi_4 = b_{nv}^2 b_{v1}^1 b_{1u}^1 b_{u2}^2 \prod_{j=2}^{m-1} b_{j(j+1)}^2. \end{aligned}$$

Remark 7. The expression of characteristic equation (14) is also obtained by using Coates flow graph method. Note that there are only five subgraphs in the flow graph of unidirectional double-ring neural network, so its characteristic equation is relatively simple, which means that the theoretical analysis of bidirectional network is more difficult than unidirectional network with the same network structure.

4.1. Asymmetric case($n \neq m$)

In this subsection, the distribution of the roots of Eq. (14) is discussed for the sake of the local stability and Hopf bifurcation of network (13) under two cases($\tau = 0$ and $\tau > 0$).

Multiplying $e^{\lambda(n+m+2)\tau}$ on both side of Eq. (14), one has

$$s^{n+m+2} - (\phi_1 + \phi_2)s^n - (\phi_3 + \phi_4)s^m = 0, \quad (15)$$

where $s = (\lambda^\alpha + a)e^{\lambda\tau}$. Since all coefficients of Eq. (15) are constants, we can define all its roots as

$$S_r^{(1)} = \xi_r^{(1)} + i\gamma_r^{(1)}, \quad r = 1, 2, \dots, n+m+2, \quad (16)$$

which actually contains $\min\{n, m\}$ zero multiple roots.

Case without time delay($\tau = 0$) For $\tau = 0$, the characteristic equation (14) is transformed into

$$(\lambda^\alpha + a)^{n+m+2} - (\phi_1 + \phi_2)(\lambda^\alpha + a)^n - (\phi_3 + \phi_4)(\lambda^\alpha + a)^m = 0, \quad (17)$$

further,

$$s^{n+m+2} - (\phi_1 + \phi_2)s^n - (\phi_3 + \phi_4)s^m = 0, \quad (18)$$

where $s = \lambda^\alpha + a$. In Section 3.1, we use the Routh–Hurwitz criterion to investigate the local stability of the networks without time delay. Although we can give the necessary conditions of the local stability, it is difficult to calculate the specific coefficients. Therefore, here we study the distribution of its roots according to the structural form of the characteristic equation.

For convenience of description, we make the hypothesis

$$(H5) : a > \max \{ \operatorname{Re}(S_r^{(1)}) \}, \quad r = 1, 2, \dots, n+m+2.$$

Then we have the following result.

Lemma 5. For $\tau = 0$, all roots of the characteristic equation (17) have negative real part when hypothesis (H5) holds. In other words, the trivial equilibrium point of network (13) without time delay is locally asymptotically stable.

Proof. Define $s_r(r = 1, 2, \dots, n+m+2)$ as the root of Eq. (17) associated with $S_r^{(1)}$, that is, $s_r^\alpha = S_r^{(1)} - a$. Since $a > \max \{ \operatorname{Re}(S_r^{(1)}) \}$ is true for all $r = 1, 2, \dots, n+m+2$, it is easy to check that $\operatorname{Re}(s_r^\alpha) \leq \max \operatorname{Re}(S_r^{(1)}) - a < 0$, which shows $|\arg(s_r^\alpha)| \geq \frac{\alpha\pi}{2}$. Hence, based on Lemma 1, the trivial equilibrium point of network (13) is locally asymptotically stable when $\tau = 0$.

Case with time delay($\tau > 0$) For $\tau > 0$, combining with $s = (\lambda^\alpha + a)e^{\lambda\tau}$ and Eq. (16), we have

$$(\lambda^\alpha + a)e^{\lambda\tau} = \xi_r^{(1)} + i\gamma_r^{(1)},$$

which has the same structure as Eq. (11), so we can use the method in Section 3.2 to analyze the local stability and Hopf bifurcation of network (13) with time delay.

4.2 Symmetrical case($n = m$)

In this subsection, we investigate the symmetric form of network (13). Namely, the number of neurons on the X -ring and Y -ring is the same, and the connection weights between neurons are uniformly defined as b . In this case, the characteristic equation (14) can be reduced to

$$(\lambda^\alpha + a)^{2n+2} - 4e^{-\lambda(n+2)\tau} b^{n+2} (\lambda^\alpha + a)^n = 0. \quad (19)$$

Case without time delay($\tau = 0$) When $\tau = 0$, Eq. (19) becomes

$$s^n (s^{n+2} - 4b^{n+2}) = 0,$$

then

$$s^{n+2} - 4b^{n+2} = 0, \quad (20)$$

in which $s = (\lambda^\alpha + a) = \rho e^{i\theta}$. It is worth noting that we can express the root of Eq. (20) on the complex plane, where ρ represents the length of s and $\theta(0 \leq \theta < 2\pi)$ is the angle of s .

Lemma 6. For $b > 0$, all roots of Eq. (20) have negative real parts when $a > \sqrt[4]{4b}$ holds, and Eq. (20) has at least one root with positive real parts when $a < \sqrt[4]{4b}$ holds.

Proof. Due to $b > 0$, one has $b^{n+2} > 0$. Hence, we have

$$s_j = \lambda_j^\alpha + a = \sqrt[4]{4b} e^{i\theta_j} = \sqrt[4]{4b} (\cos \theta_j + i \sin \theta_j),$$

in which $\theta_j = (2j\pi)/(n+2)$, $j = 0, 1, 2, \dots, n+1$. It is easy to check that s_0 is the root with the largest real part among all roots s_j , which demonstrates $\operatorname{Re}(\lambda_j^\alpha) \leq \operatorname{Re}(\lambda_0^\alpha) = \operatorname{Re}(s_0) - a = \sqrt[4]{4b} - a$ for all $j = 0, 1, 2, \dots, n+1$. Consequently, we can draw two conclusions. If

$a > \sqrt[n+2]{4}b$ is true, then $\operatorname{Re}(\lambda_j^\alpha) < 0$ implying $|\arg(\lambda_j^\alpha)| \geq \frac{\alpha\pi}{2}$, this is, all roots of Eq. (20) have negative real parts. If $a < \sqrt[n+2]{4}b$ is true, then it is obvious that there is at least one positive root $s_0 > 0$.

Lemma 7. When $b < 0$ and n is an odd number, all roots of Eq. (20) have negative real parts for $a > -\sqrt[n+2]{4}b \cos [\pi/(n+2)]$, and Eq. (20) has at least one root with positive real parts for $a < -\sqrt[n+2]{4}b \cos [\pi/(n+2)]$.

Proof. If $b < 0$ and n is an odd number, then $b^{n+2} < 0$. Thus, we have $s_j = \lambda_j^\alpha + a = -\sqrt[n+2]{4}be^{i\theta_j} = -\sqrt[n+2]{4b}(\cos \theta_j + i \sin \theta_j)$,

where $\theta_j = 2(j+1)\pi/(n+2)$, $j = 0, 1, 2, \dots, n+1$. It is easy to check that s_0 and s_{n+1} are the root with the largest real part among all roots s_j , which shows $\operatorname{Re}(\lambda_j^\alpha) \leq \operatorname{Re}(\lambda_0^\alpha) = \operatorname{Re}(s_0) - a = -\sqrt[n+2]{4b} \cos [\pi/(n+2)] - a$ for all $j = 0, 1, 2, \dots, n+1$. Clearly, if $a > -\sqrt[n+2]{4}b \cos [\pi/(n+2)]$ holds, then $\operatorname{Re}(\lambda_j^\alpha) < 0$, which implies that all roots of Eq. (20) have negative real parts. If $a < -\sqrt[n+2]{4}b \cos [\pi/(n+2)]$ holds, then it is obvious that there is at least one positive root $s_0 > 0$ or $s_{n+1} > 0$.

Lemma 8. When $b < 0$ and n is an even number, all roots of Eq. (20) have negative real parts for $a > -\sqrt[n+2]{4}b$, and Eq. (20) has at least one root with positive real parts for $a < -\sqrt[n+2]{4}b$.

Since $b < 0$ and n is an even number, it is clear that $b^{n+2} > 0$. Hence, we can use similar steps in Lemma 6 to prove Lemma 8.

Combined with Lemma 1 and Lemma 6–8, we have the following conclusion.

Theorem 2. If $a > \sqrt[n+2]{4}b$ for $b^{n+2} > 0$ or $a > -\sqrt[n+2]{4}b \cos [\pi/(n+2)]$ for $b^{n+2} < 0$ holds, then the trivial equilibrium point of symmetric network without delay is locally asymptotically stable. However, if $a < \sqrt[n+2]{4}b$ for $b^{n+2} > 0$ or $a < -\sqrt[n+2]{4}b \cos [\pi/(n+2)]$ for $b^{n+2} < 0$ holds, then the trivial equilibrium point of symmetric network without delay is unstable.

Corollary 1. For a k -ring coupled unidirectional symmetric neural network with two shared neurons, the trivial equilibrium point of the network without delay is locally asymptotically stable when $a > \sqrt[n+2]{k^2}b$ for $b^{n+2} > 0$ or $a > -\sqrt[n+2]{k^2}b \cos [\pi/(n+2)]$ for $b^{n+2} < 0$ holds and unstable when $a < \sqrt[n+2]{k^2}b$ for $b^{n+2} > 0$ or $a < -\sqrt[n+2]{k^2}b \cos [\pi/(n+2)]$ for $b^{n+2} < 0$ holds.

Case with time delay ($\tau > 0$) From Eq. (19), it is easy to obtain

$$[(\lambda^\alpha + a)e^{\lambda\tau}]^{n+2} \left\{ [(\lambda^\alpha + a)e^{\lambda\tau}]^{n+2} - 4b^{n+2} \right\} = 0,$$

by multiplying $e^{\lambda(2n+2)\tau}$ on both side of Eq. (19). Now, we consider

$$[(\lambda^\alpha + a)e^{\lambda\tau}]^{n+2} - 4b^{n+2} = 0, \quad (21)$$

and assume that $b > 0$ for generality, then Eq. (21) is rewritten as

$$(\lambda^\alpha + a)e^{\lambda\tau} = \sqrt[n+2]{4b}e^{i\theta_j} = \sqrt[n+2]{4b}(\cos \theta_j + i \sin \theta_j). \quad (22)$$

Substituting $\lambda = i\omega$ into Eq. (22) yields

$$\begin{aligned} & \left[\omega^\alpha \left(\cos \frac{\alpha\pi}{2} + i \sin \frac{\alpha\pi}{2} \right) + a \right] (\cos \omega\tau + i \sin \omega\tau) \\ &= \sqrt[n+2]{4b}(\cos \theta_j + i \sin \theta_j), \end{aligned} \quad (23)$$

where $\theta_j = (2j\pi)/(n+2)$, $j = 0, 1, 2, \dots, n+1$. Separating the real and imaginary parts of Eq. (23) leads to

$$\begin{cases} \cos \omega\tau = \frac{\sqrt[n+2]{4b} \left\{ \cos \theta_j \left(\omega^\alpha \cos \frac{\alpha\pi}{2} + a \right) + \sin \theta_j \omega^\alpha \sin \frac{\alpha\pi}{2} \right\}}{\left(\omega^\alpha \cos \frac{\alpha\pi}{2} + a \right)^2 + \left(\omega^\alpha \sin \frac{\alpha\pi}{2} \right)^2} \triangleq p_1(\omega) \\ \sin \omega\tau = \frac{\sqrt[n+2]{4b} \left\{ \sin \theta_j \left(\omega^\alpha \cos \frac{\alpha\pi}{2} + a \right) - \cos \theta_j \omega^\alpha \sin \frac{\alpha\pi}{2} \right\}}{\left(\omega^\alpha \cos \frac{\alpha\pi}{2} + a \right)^2 + \left(\omega^\alpha \sin \frac{\alpha\pi}{2} \right)^2} \triangleq q_1(\omega), \end{cases}$$

and further

$$\psi_1(\omega) \triangleq \omega^{2\alpha} + 2a\omega^\alpha \cos \frac{\alpha\pi}{2} + a^2 - \left(\sqrt[n+2]{4b} \right)^2 = 0. \quad (24)$$

For Eq. (24), we have the following lemma, whose proof idea is the same as Lemma 4.

Lemma 9. If $b > 0$ and $a < \sqrt[n+2]{4}b$ holds, then Eq. (24) has at least one positive root.

Suppose that Eq. (24) has $n+2$ different positive roots defined as ω_r , $r = 1, 2, \dots, n+2$. Then, we have

$$\tau_r^{(j)} = \frac{1}{\omega_r} \{ \arccos p_1(\omega_r) + 2j\pi \}, \quad j = 0, 1, 2, \dots$$

and $\tau_0 = \tau_{r_0}^{(0)} = \min_{r=1,\dots,n+2} \{ \tau_r^{(0)} \}$, $\omega_0 = \omega_{r_0}$. By differentiating both sides of Eq. (21) with respect to τ and then performing simple calculation, it is easy to know that when hypothesis (H4) holds, the following transversality condition is satisfied,

$$\operatorname{Re} \left(\frac{d\lambda}{d\tau} \right)_{\lambda=i\omega_0, \tau=\tau_0}^{-1} > 0.$$

Theorem 3. For the symmetric network, if hypothesis (H4), $b > 0$ and $a < \sqrt[n+2]{4}b$ are all true, then the network is locally asymptotically stable at the trivial equilibrium for $\tau \in [0, \tau_0]$, and unstable for $\tau > \tau_0$. In addition, a Hopf bifurcation occurs at the trivial equilibrium when $\tau = \tau_r^{(j)}$ for $r = 1, 2, \dots, n+2$, $j = 0, 1, 2, \dots$

Remark 8. Following Eq. (22), we have $(\lambda^\alpha + a)e^{\lambda\tau} = -\sqrt[n+2]{4b}(\cos \theta_j + i \sin \theta_j)$ when $b < 0$, in which $\theta_j = 2(j+1)\pi/(n+2)$, $j = 0, 1, 2, \dots, n+1$. Similarly, the network also undergoes Hopf bifurcation for $b < 0$ and $a < -\sqrt[n+2]{4}b$ by using the same analysis method above,

5 Numerical simulation

In this section, some numerical experiments are provided to verify the theoretical results, mainly involving the influence of connection mode, time delay, network size and fractional order on the Hopf bifurcation point of the network.

Example 1 (Bidirectional Double-Ring Model). In this experiment, we consider the following bidirectional double-ring neural network model with $n = 2$ and $m = 3$,

$$\begin{cases} D^\alpha u = -au + b_{1u}^1 \tanh(x_1) + b_{2u}^1 \tanh(x_2) + b_{1u}^2 \tanh(y_1) + b_{2u}^2 \tanh(y_2), \\ D^\alpha v = -av + b_{1v}^1 \tanh(x_1) + b_{2v}^1 \tanh(x_2) + b_{1v}^2 \tanh(y_1) + b_{2v}^2 \tanh(y_3), \\ D^\alpha x_i = -ax_i + b_{ui}^1 \tanh(u) + b_{vi}^1 \tanh(v), \\ D^\alpha y_1 = -ay_1 + b_{u1}^2 \tanh(u) + b_{v1}^2 \tanh(v), \\ D^\alpha y_2 = -ay_2 + b_{u2}^2 \tanh(u) + b_{32}^2 \tanh(y_3), \\ D^\alpha y_3 = -ay_3 + b_{23}^2 \tanh(y_2) + b_{v3}^2 \tanh(v), \end{cases} \quad (25)$$

where $i = 1, 2$ and the hyperbolic tangent function $\tanh(\cdot)$ is used as the activation function, which satisfies the hypothesis (H1) since $\tanh(0) = 0$ and $\tanh'(0) = 1$. The set of the network parameters we selected is as follows:

$$\begin{aligned} b_{1u}^1 &= 0.4, b_{2u}^1 = 0.5, b_{2u}^2 = 0.7, b_{1u}^2 = 0.2, b_{1v}^1 = 0.4, b_{2v}^1 = 0.6, b_{1v}^2 = 0.5, \\ b_{3v}^2 &= 0.3, \\ b_{u1}^1 &= -0.4, b_{v1}^1 = -0.7, b_{u2}^1 = -0.5, b_{v2}^1 = -0.6, b_{u1}^2 = -0.3, b_{v1}^2 = -0.7, \\ b_{u2}^2 &= -0.2, b_{32}^2 = -0.5, \\ b_{23}^2 &= 0.8, b_{v3}^2 = -0.6, a = 0.6, \alpha = 0.9, \end{aligned}$$

and then substituting them into Eq. (10) leads to

$$s^7 + 2.23s^5 + 0.7635s^3 - 0.0148s^2 - 0.0156s = 0,$$

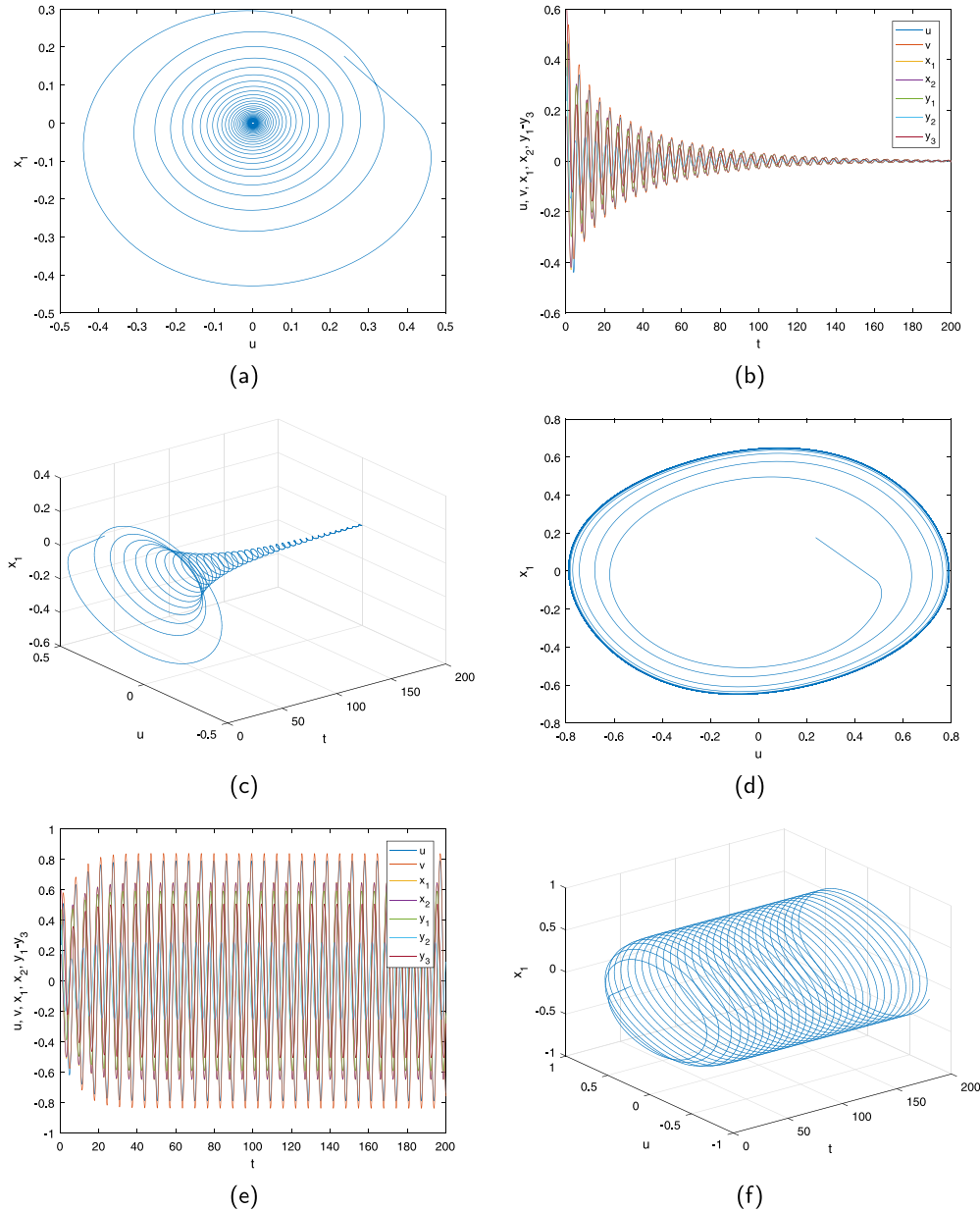


Fig. 3. Numerical results of network (25) with initial value $\phi_1(t) = 0.2$, $\phi_2(t) = 0.3$, $\phi_3(t) = 0.2$, $\phi_4(t) = 0.2$, $\phi_5(t) = 0.5$, $\phi_6(t) = 0.4$, $\phi_7(t) = 0.6$ for $t \in [-\tau, 0]$. (a)(b)(c) The trivial equilibrium point of the network is locally asymptotically stable when $\tau = 0.5$. (d)(e)(f) There is a stable periodic solution near the trivial equilibrium point when $\tau = 0.7$.

from which we can know that $\max \{ |S_r| \} \approx 1.3422$, $r = 1, 2, \dots, 7$. Due to $a = 0.6 < 1.3422$, the condition of Lemma 4 is satisfied. Hence, the critical value of Hopf bifurcation is $\tau_0 = 0.54488$ with the critical frequency $\omega_0 = 1.1234$. According to Theorem 1, when $\tau = 0.5 < \tau_0$, the trivial equilibrium point of network (25) is locally asymptotically stable, as shown in Fig. 3(a), and when $\tau = 0.7 > \tau_0$, the trivial equilibrium point becomes unstable with the appearance of stable periodic solutions, as shown in Fig. 3(d). In particular, when the time delay τ is gradually increased, the amplitude of the periodic solution of the network also becomes larger, as shown in Fig. 4. For the network without delay, it is easy to check that the conditions of Lemma 3 are satisfied under this set of parameters. Thus, the solutions from different initial values eventually converge to the trivial equilibrium point (see Fig. 5). Subsequently, we investigate the influence of fractional order, network size and the distance between two shared neurons on the Hopf bifurcation of the system, namely, the following three paragraphs.

Influence of the fractional order and self-feedback coefficient In this part, network (25) is taken as an example to analyze the influence of the fractional order and self-feedback coefficient on the Hopf bifurcation of the network. As can be seen from Fig. 6(a), in horizontal comparison, with the increase of fractional order (from 0.2 to 1), the first Hopf bifurcation point of the network gradually decreases, that is, a larger fractional order will make the Hopf bifurcation occur in advance. In addition, through longitudinal comparison, it can be found that the increase of the self-feedback coefficient will delay the Hopf bifurcation of the network. For the critical frequency ω_0 , its variation is just opposite to that of Hopf bifurcation point τ_0 (see Fig. 6(b)).

Influence of the number of total neurons In this part, we investigate the influence of the number of total neurons the network on the Hopf bifurcation. In order to eliminate the difference in experimental results caused by the parameters, all the connection weights here are uniformly set to $b = 0.5$. The growth mode of the number of total

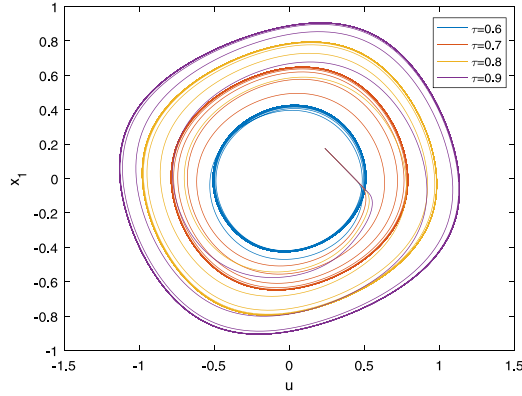


Fig. 4. With the increase in the time delay τ , the periodic amplitude of Hopf bifurcation becomes larger and larger with initial value $\phi_1(t) = 0.2$, $\phi_2(t) = 0.3$, $\phi_3(t) = 0.2$, $\phi_4(t) = 0.2$, $\phi_5(t) = 0.5$, $\phi_6(t) = 0.4$, $\phi_7(t) = 0.6$ for $t \in [-\tau, 0]$.

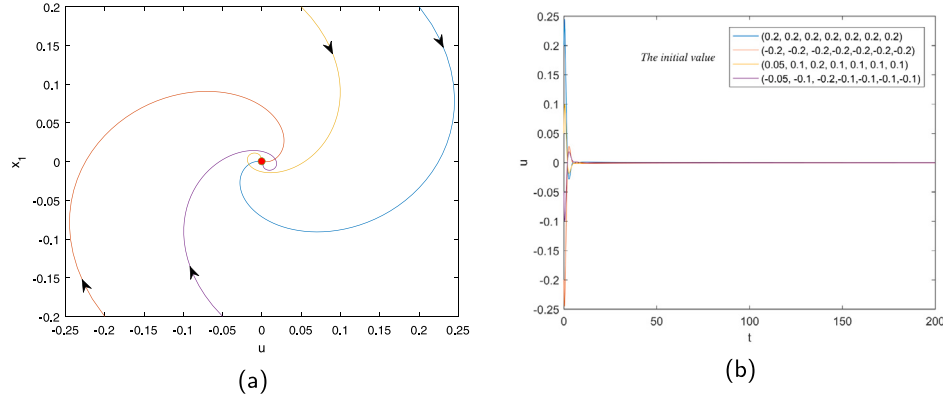


Fig. 5. Numerical results of network (25) with $\tau = 0$. (a) All solutions of the system eventually converge to the trivial equilibrium point. (b) The waveform diagram corresponding to (a).

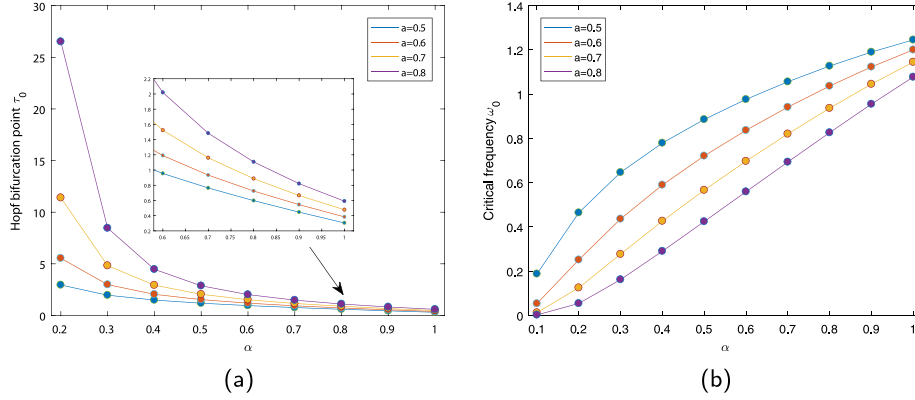


Fig. 6. The influence of fractional order and self-feedback coefficient on Hopf bifurcation point τ_0 and critical frequency ω_0 of the network.

neurons in the network is defined as follows:

$$(n, m) : (2, 2) \rightarrow (2, 3) \rightarrow (3, 3) \rightarrow (3, 4) \rightarrow (4, 4) \rightarrow (4, 5) \rightarrow \dots .$$

The experimental results are shown in Table 1, from which we can see that with the increase in the number of total neurons of the network, the Hopf bifurcation point τ_0 also gradually increases, indicating that large-scale networks will inhibit the emergence of Hopf bifurcation.

Influence of the distance between two shared neurons In this part, we choose a bidirectional double-ring neural network with 10 neurons in

each ring to study the influence of the distance between two shared neurons on the Hopf bifurcation of the network. It can be seen from Table 2 that when two shared neurons are closest, that is, there are no other neurons between them, the Hopf bifurcation point τ_0 is the largest, but with the increase in the distance (from $d = 1$ to $d = 5$), τ_0 shows an increasing trend in a small range.

Example 2 (Unidirectional Double-ring Model). In this example, we investigate the unidirectional double-ring model corresponding to the

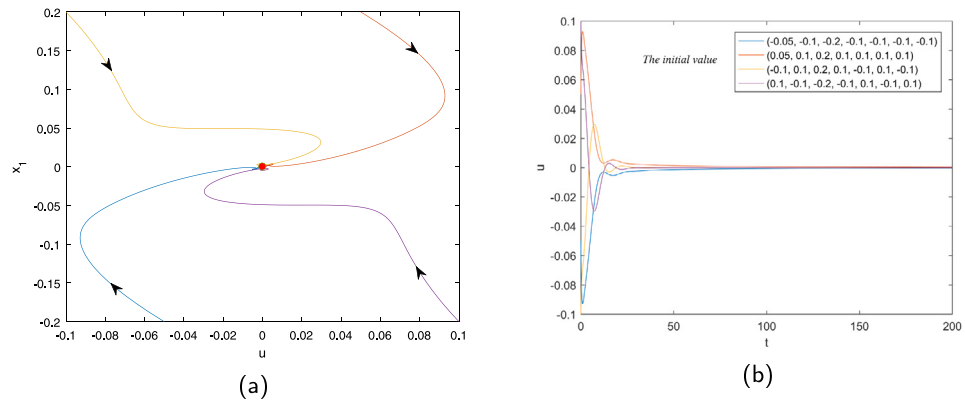


Fig. 7. Numerical results of network (26) with $\tau = 0$. (a) All solutions of the system eventually converge to the trivial equilibrium point. (b) The waveform diagram corresponding to (a).

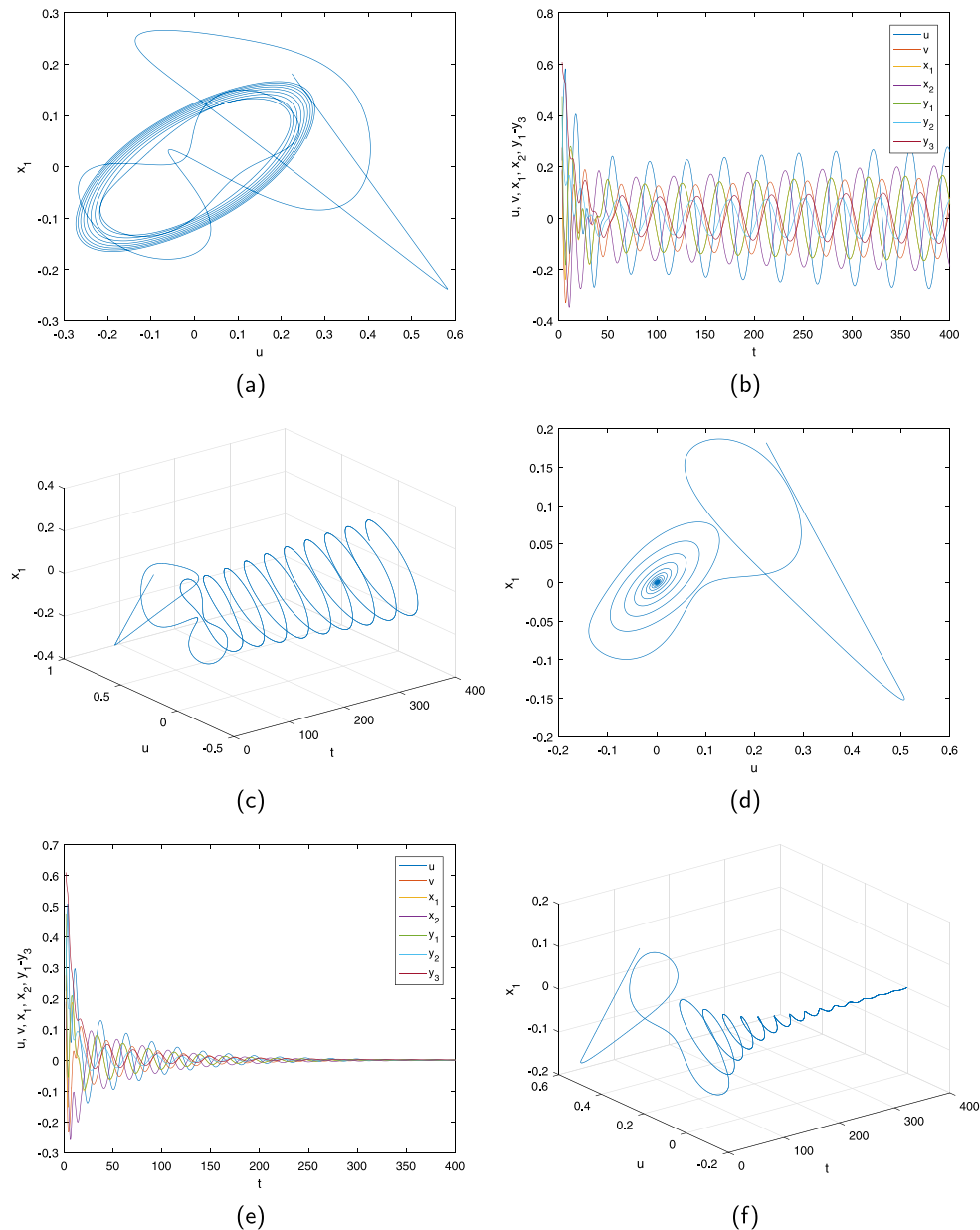


Fig. 8. Numerical results of network (26) with initial value $\phi_1(t) = 0.2$, $\phi_2(t) = 0.3$, $\phi_3(t) = 0.2$, $\phi_4(t) = 0.2$, $\phi_5(t) = 0.5$, $\phi_6(t) = 0.4$, $\phi_7(t) = 0.6$ for $t \in [-\tau, 0]$. (a)(b)(c) There is an unstable periodic solution near the trivial equilibrium point when $\tau = 3.3$. (d)(e)(f) The trivial equilibrium point of the network is locally asymptotically stable when $\tau = 1.8$.

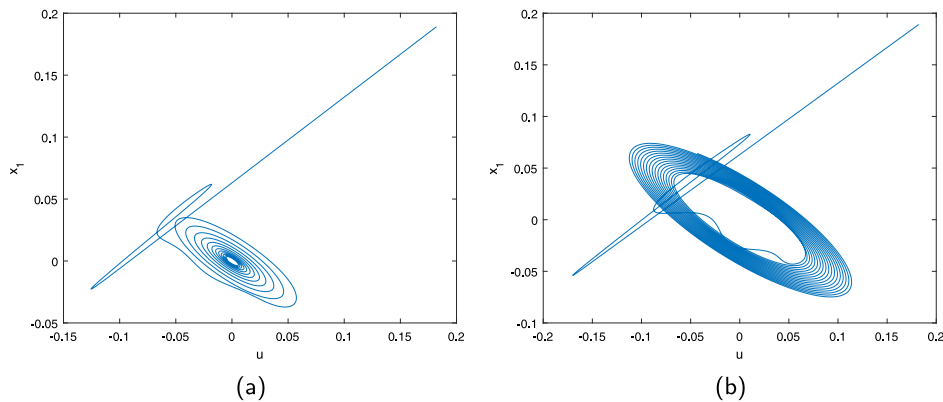


Fig. 9. Numerical results of the network with initial value $\phi_1(t) = 0.2$, $\phi_2(t) = 0.2$, $\phi_3(t) = 0.2$, $\phi_4(t) = 0.2$, $\phi_5(t) = 0.2$, $\phi_6(t) = 0.2$, $\phi_7(t) = 0.2$, $\phi_8(t) = 0.2$ for $t \in [-\tau, 0]$. (a) The trivial equilibrium point of the network is locally asymptotically stable when $\tau = 1.5$, $a = 0.6$ and $b = -0.5$. (b) There is an unstable periodic solution near the trivial equilibrium point when $\tau = 2.1$, $a = 0.6$ and $b = -0.5$.

Table 1

The influence of the number of total neurons on the Hopf bifurcation of the network.

X-ring	Y-ring	Total neurons	Hopf point τ_0
$n = 2$	$m = 2$	$n + m + 2 = 6$	0.80871
$n = 2$	$m = 3$	$n + m + 2 = 7$	0.83090
$n = 3$	$m = 3$	$n + m + 2 = 8$	0.85227
$n = 3$	$m = 4$	$n + m + 2 = 9$	0.86315
$n = 4$	$m = 4$	$n + m + 2 = 10$	0.87411
$n = 4$	$m = 5$	$n + m + 2 = 11$	0.87973
\vdots	\vdots	\vdots	\vdots
$n = 10$	$m = 10$	$n + m + 2 = 22$	0.8971

Table 2

The influence of the distance between two shared neurons on the Hopf bifurcation of the network, where d represents the number of neurons between two shared neurons.

Hopf point	Dis					
	$d = 0$	$d = 1$	$d = 2$	$d = 3$	$d = 4$	$d = 5$
τ_0	1.01675	0.8971	0.9351	0.9544	0.9639	0.9668

network (25),

$$\left\{ \begin{array}{l} D^\alpha u = -au + b_{1u}^1 \tanh(x_1) + b_{1u}^2 \tanh(y_1), \\ D^\alpha v = -av + b_{2v}^1 \tanh(x_2) + b_{3v}^2 \tanh(y_3), \\ D^\alpha x_1 = -ax_1 + b_{v1}^1 \tanh(v), \\ D^\alpha x_2 = -ax_2 + b_{u2}^1 \tanh(u), \\ D^\alpha y_1 = -ay_1 + b_{v1}^2 \tanh(v), \\ D^\alpha y_2 = -ay_2 + b_{u2}^2 \tanh(u), \\ D^\alpha y_3 = -ay_3 + b_{23}^2 \tanh(y_2), \end{array} \right. \quad (26)$$

where the values of system parameters are selected as follows,

$$\begin{aligned} b_{1u}^1 &= 0.4, b_{1u}^2 = 0.7, b_{2v}^1 = -0.6, b_{3v}^2 = -0.3, b_{v1}^1 = -0.7, \\ b_{u2}^1 &= -0.5, b_{v1}^2 = -0.7, b_{u2}^2 = 0.2, b_{23}^2 = 0.8, a = 0.6, \alpha = 0.9. \end{aligned}$$

Thus, Eq. (15) is reduced to

$$s^7 + 0.231s^3 - 0.037s^2 = 0,$$

then $\max \{ \operatorname{Re}(S_r^{(1)}) \} \approx 0.4465$, $r = 1, 2, \dots, 7$. When $\tau = 0$, it is easy to check by Lemma 5 that network (26) is locally asymptotically stable for $a = 0.6 > 0.4465$ (see Fig. 7). Moreover, for $\tau > 0$, similar to Example 1, the critical value $\tau_0 = 2.88839$ with the critical frequency $\omega_0 = 0.1791$ of Hopf bifurcation can be obtained. Hence, when $\tau = 1.8 < \tau_0$, the network (26) is locally asymptotically stable at the trivial equilibrium point (see Fig. 8(d)), and when $\tau = 3.3 > \tau_0$, the network becomes unstable and periodic solutions appear near the trivial equilibrium

point (see Fig. 8(a)). Now, the stability and Hopf bifurcation of the symmetric network and the comparison between unidirectional and bidirectional double-ring network are discussed in the following two paragraphs.

Symmetric network We unify all connection weights as $b = 0.5$ and self-feedback coefficient $a = 0.6$ to investigate the stability and Hopf bifurcation of symmetric networks when n is an even or odd number. As can be seen from Table 3, when $n = 2, 3, 4, 5$, the conditions of Lemma 7 and Lemma 8 are satisfied, and the network undergoes a Hopf bifurcation, while when $n > 5$, the network is always stable. We take $n = 3$ as an example to show the dynamic properties of the network near the Hopf bifurcation point. For $\tau = 1.5 < \tau_0$, the trivial equilibrium point of the network is locally asymptotically stable (see Fig. 9(a)). For $\tau = 2.1 > \tau_0$, there is an unstable periodic solution near the trivial equilibrium point (see Fig. 9(b)).

Influence of the unidirectional and bidirectional connection We unify all connection weights as $b = 0.5$ to compare the influence of bidirectional and unidirectional connections on the Hopf bifurcation of the network. It can be seen from Table 4 that in general, the bidirectional connection promotes the appearance of the Hopf bifurcation, while the unidirectional connection network delays the Hopf bifurcation.

Remark 9. The results are of practical significance. On the one hand, understanding the dynamic behavior of the entire network is very important for studying the interconnection patterns occurring in complex networks, which is called “network motifs” [32]. On the other hand, the theoretical results can be used to analyze the stability of practical networks, for example, adjust the information transmission(unidirection or bidirection) and coupling mode (such as the distance between two shared neurons in this paper) to make the network stable or strengthen its stable region. In our future work, we will attempt to find the real-data and carry out numerical experiments on the real-data set.

6 Conclusion and discussion

In this paper, we propose a double-ring neural network model with two shared neurons and multiple delays, in which both unidirectional and bidirectional connection are considered. The stability and Hopf bifurcation of the network are investigated via the characteristic equation induced by the flow graph theory at the trivial equilibrium point. Finally, some numerical experiments show the validity of the theoretical results. In addition, the Hopf bifurcation of the double-ring neural network with large fractional order, a small number of neurons and a bidirectional connection mode will appear ahead of time in contrast

Table 3The stability and Hopf bifurcation of the network with $a = 0.6$, $b = 0.5$.

Number of neurons	$a - \sqrt[ns]{4b}$	τ_0	ω_0	Stability/Instability
$n = 2$	$-0.1071 < 0$	1.6497	0.2546	Hopf bifurcation
$n = 3$	$-0.0598 < 0$	1.8209	0.1636	Hopf bifurcation
$n = 4$	$-0.030 < 0$	1.9965	0.0946	Hopf bifurcation
$n = 5$	$-0.0095 < 0$	2.2697	0.03476	Hopf bifurcation
$n = 6$	$0.0054 > 0$	/	/	Stable
$n = 7$	$0.0167 > 0$	/	/	Stable
$n = 8$	$0.0257 > 0$	/	/	Stable
$n = 9$	$0.0328 > 0$	/	/	Stable
$n = 10$	$0.0388 > 0$	/	/	Stable

Table 4

The influence of the connection mode on the Hopf bifurcation of the network.

X-ring	Y-ring	Total neurons	Bidirectional τ_0	Unidirectional τ_0
$n = 2$	$m = 2$	$n + m + 2 = 6$	0.79111	1.6496
$n = 2$	$m = 3$	$n + m + 2 = 7$	0.81336	1.7307
$n = 3$	$m = 3$	$n + m + 2 = 8$	0.83502	1.8207
$n = 3$	$m = 4$	$n + m + 2 = 9$	0.84609	1.8996
$n = 4$	$m = 4$	$n + m + 2 = 10$	0.85721	9.054
$n = 4$	$m = 5$	$n + m + 2 = 11$	0.86300	2.10

to the network with small fractional order, a large number of neurons and a unidirectional connection. Inspired by the double-ring model, our future work will focus on multi-ring coupled neural networks, and more complex dynamic phenomena, such as co-dimension two bifurcations, chaotic behavior and network synchronization, will also be studied.

CRediT authorship contribution statement

Qinrui Dai: Conceptualization, Methodology, Writing – review & editing.

Declaration of competing interest

The authors declare that they have no known competing financial interests or personal relationships that could have appeared to influence the work reported in this paper.

Data availability

No data was used for the research described in the article.

Acknowledgments

The author is grateful to all anonymous reviewers for their valuable comments, which has provided great help for the improvement of the paper.

Appendix

The parameters of the subgraph

$$\begin{aligned} \varphi_1^{(1)} &= \sum_{i_1=1}^{n+2} c_{i_1} + \sum_{j_1=1}^{m+2} d_{j_1}, \\ \varphi_2^{(1)} &= \sum_{i_1=3}^{n+1} (c_1 + d_1 + d_2)c_{i_1} + \sum_{i_1=2}^n \sum_{i_2=i_1+2}^{n+2} c_{i_1}c_{i_2} + \sum_{j_1=3}^{m+1} d_1d_{j_1} \\ &\quad + \sum_{j_1=2}^m \sum_{j_2=j_1+2}^{m+2} d_{j_1}d_{j_2} + \sum_{i_1=2}^n (d_{m+1} + d_{m+2})c_{i_1} \\ &\quad + \sum_{j_2=3}^m \sum_{i_2=1}^{n+1} d_{j_2}c_{i_2}, \end{aligned}$$

$$\begin{aligned} \varphi_3^{(1)} &= \sum_{i_1=2}^{n-1} \sum_{i_2=i_1+2}^{n+1} c_1c_{i_1}c_{i_2} + \sum_{i_1=2}^{n-2} \sum_{i_2=i_1+2}^n \sum_{i_3=i_2+2}^{n+2} c_{i_1}c_{i_2}c_{i_3} \\ &\quad + \sum_{j_1=2}^{m-1} \sum_{j_2=j_1+2}^{m+1} d_1d_{j_1}d_{j_2} \\ &\quad + \sum_{j_1=2}^{m-2} \sum_{j_2=j_1+2}^m \sum_{j_3=j_2+2}^{m+2} d_{j_1}d_{j_2}d_{j_3} \\ &\quad + \sum_{j_1=3}^m \sum_{j_2=j_1+2}^{m+2} (c_1 + c_2)d_{j_1}d_{j_2} + \sum_{i_1=3}^n \sum_{i_2=i_1+2}^{n+2} (d_1 + d_2)c_{i_1}c_{i_2} \\ &\quad + \sum_{i_1=3}^n \sum_{i_2=i_1+2}^{m+2} c_{i_1}d_{j_2}d_{j_3} \\ &\quad + \sum_{i_1=3}^n \sum_{i_2=i_1+2}^{n+2} (d_1 + d_2)c_{i_1}c_{i_2} + \sum_{j_1=2}^{m-2} \sum_{j_2=j_1+2}^m (c_{n+1} + c_{n+2})d_{j_1}d_{j_2} \\ &\quad + \sum_{i_1=2}^{n-2} \sum_{i_2=i_1+2}^n (d_{m+1} + d_{m+2})c_{i_1}c_{i_2} \\ &\quad + \sum_{j_1=3}^m \sum_{i_2=i_1+2}^{n+2} d_{j_1}c_{i_1}c_{i_2} \\ &\quad + \vdots \\ \varphi_k^{(1)} &= \sum_{i_2=2}^{n+5-2k} \cdots \sum_{i_{k-1}=i_{k-2}+2}^{n-1} \sum_{i_k=i_{k-1}+2}^{n+1} c_1c_{i_2} \cdots c_{i_{k-1}}c_{i_k} \\ &\quad + \sum_{i_1=2}^{n+4-2k} \sum_{i_2=i_1+2}^{n+8-2k} \cdots \sum_{i_{k-1}=i_{k-2}+2}^n \sum_{i_k=i_{k-1}+2}^{n+2} c_{i_1}c_{i_2} \cdots c_{i_{k-1}}c_{i_k} \\ &\quad + \sum_{j_2=2}^{m+5-2k} \cdots \sum_{j_{k-1}=j_{k-2}+2}^{m-1} \sum_{j_k=j_{k-1}+2}^{m+1} d_1d_{j_2} \cdots d_{j_{k-1}}d_{j_k} \\ &\quad + \sum_{j_1=2}^{m+4-2k} \sum_{j_2=j_1+2}^{m+8-2k} \cdots \sum_{j_{k-1}=j_{k-2}+2}^m \sum_{j_k=j_{k-1}+2}^{m+2} d_{j_1}d_{j_2} \cdots d_{j_{k-1}}d_{j_k} \\ &\quad + \sum_{j_1=3}^{m+6-2k} \sum_{j_2=j_1+2}^{m+10-2k} \cdots \sum_{j_{k-1}=j_{k-2}+2}^{m+2} (c_1 + c_2)d_{j_1}d_{j_2} \cdots d_{j_{k-1}} \\ &\quad + \sum_{j_1=2}^{m+4-2k} \sum_{j_2=j_1+2}^{m+8-2k} \cdots \sum_{j_{k-1}=j_{k-2}+2}^m (c_{n+1} + c_{n+2})d_{j_1}d_{j_2} \cdots d_{j_{k-1}} \\ &\quad + \sum_{i_1=3}^{n+6-2k} \sum_{j_1=2}^{m+6-2k} \sum_{j_2=j_1+2}^{m+10-2k} \cdots \sum_{j_{k-1}=j_{k-2}+2}^{m+2} c_{i_1}d_{j_1}d_{j_2} \cdots d_{j_{k-1}} \\ &\quad + \sum_{i_1=3}^{n+6-2k} \sum_{i_2=i_1+2}^{n+10-2k} \cdots \sum_{i_{k-1}=i_{k-2}+2}^{n+2} (d_1 + d_2)c_{i_1}c_{i_2} \cdots c_{i_{k-1}} \\ &\quad + \sum_{i_1=2}^{n+4-2k} \sum_{i_2=i_1+2}^{n+8-2k} \cdots \sum_{i_{k-1}=i_{k-2}+2}^n (d_{m+1} + d_{m+2})c_{i_1}c_{i_2} \cdots c_{i_{k-1}} \\ &\quad + \sum_{j_1=3}^{m+6-2k} \sum_{i_1=2}^{n+6-2k} \sum_{i_2=i_1+2}^{n+10-2k} \cdots \sum_{i_{k-1}=i_{k-2}+2}^{n+2} d_{j_1}c_{i_1}c_{i_2} \cdots c_{i_{k-1}} + \cdots, \end{aligned}$$

$$\begin{aligned}\varphi_1^{(2)} &= c_1 d_1 c_{n+2} d_{m+2} \left(\sum_{i_1=3}^n c_{i_1} + \sum_{j_1=3}^m d_{j_1} \right), \\ \varphi_2^{(2)} &= c_1 d_1 c_{n+2} d_{m+2} \left(\sum_{i_1=3}^{n-2} \sum_{i_2=i_1+2}^n c_{i_1} c_{i_2} \right. \\ &\quad \left. + \sum_{j_1=3}^{m-2} \sum_{j_2=j_1+2}^m d_{j_1} d_{j_2} + \sum_{i_1=3}^n \sum_{j_1=3}^m c_{i_1} d_{j_1} \right), \\ \varphi_3^{(2)} &= c_1 d_1 c_{n+2} d_{m+2} \left(\sum_{i_1=2}^{n-4} \sum_{i_2=i_1+2}^{n-2} \sum_{i_3=i_2+2}^n c_{i_1} c_{i_2} c_{i_3} \right. \\ &\quad \left. + \sum_{j_1=2}^{m-4} \sum_{j_2=j_1+2}^{m-2} \sum_{j_3=j_2+2}^m d_{j_1} d_{j_2} d_{j_3} \right. \\ &\quad \left. + \sum_{i_1=3}^n \sum_{j_2=3}^{m-2} \sum_{j_3=j_2+2}^m c_{i_1} d_{j_2} d_{j_3} + \sum_{j_1=3}^m \sum_{i_2=3}^{n-2} \sum_{i_3=i_2+2}^n d_{j_1} c_{i_2} c_{i_3} \right), \\ &\vdots\end{aligned}$$

$$\begin{aligned}\varphi_{k-1}^{(2)} &= c_1 d_1 c_{n+2} d_{m+2} \left(\sum_{i_1=3}^{n+4-2k} \sum_{i_2=i_1+2}^{n+8-2k} \cdots \sum_{i_{k-1}=i_{k-2}+2}^n c_{i_1} c_{i_2} \cdots c_{i_{k-1}} \right. \\ &\quad \left. + \sum_{i_1=3}^n \sum_{j_1=3}^{m+6-2k} \cdots \sum_{j_{k-2}=j_{k-3}+2}^m c_{i_1} d_{j_1} \cdots d_{j_{k-2}} \right. \\ &\quad \left. + \sum_{j_1=3}^m \sum_{i_1=3}^{n+6-2k} \cdots \sum_{i_{k-2}=i_{k-3}+2}^n d_{j_1} c_{i_1} \cdots c_{i_{k-2}} \right. \\ &\quad \left. + \sum_{j_1=3}^{m+4-2k} \sum_{j_2=j_1+2}^{m+8-2k} \cdots \sum_{j_{k-1}=j_{k-2}+2}^m d_{j_1} d_{j_2} \cdots d_{j_{k-1}} \right), \\ \varphi_0^{(3)} &= \prod_{i_1=1}^{n+2} c_{i_1} + (b_{u1}^1 b_{1v}^1 b_{2u}^1 b_{vn}^1 + b_{u1}^2 b_{1v}^2 b_{2u}^1 b_{vn}^1) \prod_{i=3}^n b_{i(i-1)}^1 + d_1 d_{m+2} \prod_{i_1=2}^{n+1} c_{i_1}, \\ \varphi_1^{(3)} &= \left(\prod_{i_1=1}^{n+2} c_{i_1} + (b_{u1}^1 b_{1v}^1 b_{2u}^1 b_{vn}^1 + b_{u1}^2 b_{1v}^2 b_{2u}^1 b_{vn}^1) \prod_{i=3}^n b_{i(i-1)}^1 \right. \\ &\quad \left. + d_1 d_{m+2} \prod_{i_1=2}^{n+1} c_{i_1} \right) \sum_{j_1=3}^m d_{j_1}, \\ \varphi_2^{(3)} &= \left(\prod_{i_1=1}^{n+2} c_{i_1} + (b_{u1}^1 b_{1v}^1 b_{2u}^1 b_{vn}^1 + b_{u1}^2 b_{1v}^2 b_{2u}^1 b_{vn}^1) \prod_{i=3}^n b_{i(i-1)}^1 \right. \\ &\quad \left. + d_1 d_{m+2} \prod_{i_1=2}^{n+1} c_{i_1} \right) \sum_{j_1=3}^{m-2} \sum_{j_2=j_1+2}^m d_{j_1} d_{j_2}, \\ &\vdots \\ \varphi_{k_1}^{(3)} &= \left(\prod_{i_1=1}^{n+2} c_{i_1} + (b_{u1}^1 b_{1v}^1 b_{2u}^1 b_{vn}^1 + b_{u1}^2 b_{1v}^2 b_{2u}^1 b_{vn}^1) \prod_{i=3}^n b_{i(i-1)}^1 \right. \\ &\quad \left. + d_1 d_{m+2} \prod_{i_1=2}^{n+1} c_{i_1} \right) \\ &\quad \times \sum_{j_1=3}^{m+2-2k_1} \cdots \sum_{j_{k_1-1}=j_{k_1-2}+2}^{m-2} \sum_{j_{k_1}=j_{k_1-1}+2}^m d_{j_1} d_{j_2} \cdots d_{j_{k_1-1}} d_{j_{k_1}}, \\ \varphi_0^{(4)} &= \prod_{j_1=1}^{m+2} d_{j_1} + (b_{u1}^2 b_{1v}^2 b_{2u}^2 b_{vn}^2 + b_{u1}^1 b_{1v}^1 b_{2u}^2 b_{vn}^2) \prod_{j=3}^m b_{j(j-1)}^2 + c_1 c_{n+2} \prod_{j_1=2}^{m+1} d_{j_1}, \\ \varphi_1^{(4)} &= \left(\prod_{j_1=1}^{m+2} d_{j_1} + (b_{u1}^2 b_{1v}^2 b_{2u}^2 b_{vn}^2 + b_{u1}^1 b_{1v}^1 b_{2u}^2 b_{vn}^2) \prod_{j=3}^m b_{j(j-1)}^2 \right. \\ &\quad \left. + c_1 c_{n+2} \prod_{j_1=2}^{m+1} d_{j_1} \right) \sum_{i_1=3}^n c_{i_1}, \\ \varphi_2^{(4)} &= \left(\prod_{j_1=1}^{m+2} d_{j_1} + (b_{u1}^2 b_{1v}^2 b_{2u}^2 b_{vn}^2 + b_{u1}^1 b_{1v}^1 b_{2u}^2 b_{vn}^2) \prod_{j=3}^m b_{j(j-1)}^2 \right)\end{aligned}$$

$$\begin{aligned}&\quad + c_1 c_{n+2} \prod_{j_1=2}^{m+1} d_{j_1} \right) \sum_{i_1=3}^{n-2} \sum_{i_2=i_1+2}^n c_{i_1} c_{i_2}, \\ &\quad \vdots \\ \varphi_{k_2}^{(4)} &= \left(\prod_{j_1=1}^{m+2} d_{j_1} + (b_{u1}^2 b_{1v}^2 b_{2u}^2 b_{vn}^2 + b_{u1}^1 b_{1v}^1 b_{2u}^2 b_{vn}^2) \prod_{j=3}^m b_{j(j-1)}^2 \right. \\ &\quad \left. + c_1 c_{n+2} \prod_{j_1=2}^{m+1} d_{j_1} \right) \\ &\quad \times \sum_{i_1=3}^{n+2-2k_1} \cdots \sum_{i_{k_2-1}=j_{k_2-2}+2}^{n-2} \sum_{j_{k_2}=j_{k_2-1}+2}^n c_{i_1} c_{i_2} \cdots c_{i_{k_2-1}} c_{i_{k_2}}, \\ \varphi_1^{(5)} &= b_{uv}^1 b_{u2}^1 \prod_{i_1=3}^n c_{i_1} + b_{vm}^2 b_{2u}^2 \prod_{j_1=3}^m d_{j_1} + b_{vn}^1 b_{2u}^1 \prod_{i=3}^n b_{i(i-1)}^1 \\ &\quad + b_{mv}^2 b_{u2}^2 \prod_{j=3}^m b_{j(j-1)}^1.\end{aligned}$$

References

- [1] Tang Ying, Elhoseny Mohamed. Computer network security evaluation simulation model based on neural network. *J Intell Fuzzy Syst* 2019;37(3):3197–204.
- [2] Wang Zeli, Li Heng, Zhang Xiaoling. Construction waste recycling robot for nails and screws: Computer vision technology and neural network approach. *Automat Construct* 2019;97:220–8.
- [3] Vyacheslavovich Buzaev Igor, Vyacheslavovich Plechev Vladimir, Evgenievna Nikolaeva Irina, Maratovna Galimova Rezida. Artificial intelligence: Neural network model as the multidisciplinary team member in clinical decision support to avoid medical mistakes. *Chronis Dis Transl Med* 2016.
- [4] Hirasawa Toshiaki, Aoyama Kazuharu, Tanimoto Tetsuya, Ishihara Soichiro, Shichijo Satoki, Ozawa Tsuyoshi, Ohnishi Tatsuya, Fujishiro Mitsuhiro, Matsuo Keigo, Fujisaki Junko, et al. Application of artificial intelligence using a convolutional neural network for detecting gastric cancer in endoscopic images. *Gastric Cancer* 2018;21(4):653–60.
- [5] Hudson Donna L, Cohen Maurice E. Neural networks and artificial intelligence for biomedical engineering. Wiley Online Library; 2000.
- [6] Dudhagara Dushyant R, Rajpara Rahul K, Bhatt Jwalant K, Gosai Haren B, Dave Bharti P. Bioengineering for polycyclic aromatic hydrocarbon degradation by Mycobacterium litorale: Statistical and artificial neural network (ANN) approach. *Chem Intell Lab Syst* 2016;159:155–63.
- [7] Hao Zhang, Xing-yuan Wang, Xiao-hui Lin. Synchronization of complex-valued neural network with sliding mode control. *J Frank Inst* 2016;353(2):345–58.
- [8] Yu Wenwu, Cao Jinde, Chen Guanrong. Stability and Hopf bifurcation of a general delayed recurrent neural network. *IEEE Trans Neural Netw* 2008;19(5):845–54.
- [9] Lin Hairong, Wang Chunhua, Tan Yumei. Hidden extreme multistability with hyperchaos and transient chaos in a Hopfield neural network affected by electromagnetic radiation. *Nonlinear Dynam* 2020;99(3):2369–86.
- [10] Yu Juan, Hu Cheng, Jiang Haijun. α -Stability and α -synchronization for fractional-order neural networks. *Neural Netw* 2012;35:82–7.
- [11] Xu Changjin, Zhang Wei, Liu Zixin, Yao Lingyun. Delay-induced periodic oscillation for fractional-order neural networks with mixed delays. *Neurocomputing* 2022;488:681–93.
- [12] Huang Chengdai, Cao Jinde. Bifurcations induced by self-connection delay in high-order fractional neural networks. *Neural Process Lett* 2021;53(1):637–51.
- [13] Wang Yangling, Cao Jinde, Huang Chengdai. Exploration of bifurcation for a fractional-order BAM neural network with $n+2$ neurons and mixed time delays. *Chaos Solitons Fractals* 2022;159:112117.
- [14] Eccles John C. The cerebellum as a neuronal machine. Springer Science & Business Media; 2013.
- [15] Kim Sang-Yoon, Lim Woochang. Effect of diverse recoding of granule cells on optokinetic response in a cerebellar ring network with synaptic plasticity. *Neural Netw* 2021;134:173–204.
- [16] Wang Ling, Zhao Hongyong, Cao Jinde. Synchronized bifurcation and stability in a ring of diffusively coupled neurons with time delay. *Neural Netw* 2016;75:32–46.
- [17] Song Yongli, Han Yanyan, Peng Yahong. Stability and Hopf bifurcation in an unidirectional ring of n neurons with distributed delays. *Neurocomputing* 2013;121:442–52.
- [18] Tao Binbin, Xiao Min, Zheng Wei Xing, Cao Jinde, Tang Jingwen. Dynamics analysis and design for a bidirectional super-ring-shaped neural network with n neurons and multiple delays. *IEEE Trans Neural Netw Learn Syst* 2020;32(7):2978–92.

- [19] Li Shuai, Huang Chengdai, Yuan Sanling. Hopf bifurcation of a fractional-order double-ring structured neural network model with multiple communication delays. *Nonlinear Dynam* 2022;108(1):379–96.
- [20] Zhang Yuezhong, Xiao Min, Zheng Wei Xing, Cao Jinde. Large-scale neural networks with asymmetrical three-ring structure: Stability, nonlinear oscillations, and hopf bifurcation. *IEEE Trans Cybern* 2021.
- [21] Zhang Yuezhong, Xiao Min, Cao Jinde, Zheng Wei Xing. Dynamical bifurcation of large-scale-delayed fractional-order neural networks with hub structure and multiple rings. *IEEE Trans Syst, Man, Cybern: Syst* 2020.
- [22] Zhou Shuai, Xiao Min, Wang Lu, Cheng Zunshui. Bifurcation and oscillations of a multi-ring coupling neural network with discrete delays. *Cogn Comput* 2021;13(5):1233–45.
- [23] Xing Ruitao, Xiao Min, Zhang Yuezhong, Qiu Jianlong. Stability and Hopf bifurcation analysis of an $(n+m)$ -neuron double-ring neural network model with multiple time delays. *J Syst Sci Complex* 2022;35(1):159–78.
- [24] Mazrooei-Sebdani Reza, Farjami Saeed. On a discrete-time-delayed Hopfield neural network with ring structures and different internal decays: bifurcations analysis and chaotic behavior. *Neurocomputing* 2015;151:188–95.
- [25] Wu Jie, Zhao Chongyan, Jin Nan, He Shuaibiao, Ma Dianguang. Bidirectional information transmission in SWIPT system with single controlled chopper receiver. *Electron* 2019;8(9):1027.
- [26] Vicente Raúl, Mirasso Claudio R, Fischer Ingo. Simultaneous bidirectional message transmission in a chaos-based communication scheme. *Opt Lett* 2007;32(4):403–5.
- [27] Ji Li, Wang Lifang, Liao Chenglin, Li Shufan. Simultaneous wireless power and bidirectional information transmission with a single-coil, dual-resonant structure. *IEEE Trans Ind Electron* 2018;66(5):4013–22.
- [28] Sar Emrullah Ya, Giresunlu İlker Burak. Fractional differential equations. *Pramana-J Phys* 2016;87:17.
- [29] Deng Weihua, Li Changpin, Lü Jinhu. Stability analysis of linear fractional differential system with multiple time delays. *Nonlinear Dynam* 2007;48(4):409–16.
- [30] Desoer Charles A. The optimum formula for the gain of a flow graph or a simple derivation of Coates' formula. *Proceed IRE* 1960;48(5):883–9.
- [31] Chen Jing, Xiao Min, Wan Youhong, Huang Chengdai, Xu Fengyu. Dynamical bifurcation for a class of large-scale fractional delayed neural networks with complex ring-hub structure and hybrid coupling. *IEEE Trans Neural Netw Learn Syst* 2021.
- [32] Milo Ron, Shen-Orr Shai, Itzkovitz Shalev, Kashtan Nadav, Chklovskii Dmitri, Alon Uri. Network motifs: simple building blocks of complex networks. *Science* 2002;298(5594):824–7.